OPEN ACCESS

Original research

Novel IL-4/HB-EGF-dependent crosstalk between eosinophils and macrophages controls liver regeneration after ischaemia and reperfusion injury

Yang Yang ,[1] Long Xu,[1] Constance Atkins,[1] Lily Kuhlman,[2] Jie Zhao,[1] Jong-Min Jeong,[1] Yankai Wen,[2] Nicolas Moreno,[1] Kang Ho Kim,[1] Yu A An,[1] Fenfen Wang,[1] Steve Bynon,[3] Vincenzo Villani,[3] Bin Gao ,[4] Frank Brombacher,[5] Raymond Harris,[6] Holger K Eltzschig,[1] Elizabeth Jacobsen,[7] Cynthia Ju [1]

► Additional supplemental material is published online only. To view, please visit the journal online (https://doi.org/10.1136/gutjnl-2024-332033).

For numbered affiliations see end of article.

Correspondence to
Dr Cynthia Ju, Department of Anesthesiology, Critical Care and Pain Medicine, McGovern Medical School, University of Texas Health Science Center at Houston, Houston, TX, USA; changqing.ju@uth.tmc.edu

YY and LX contributed equally.

Received 22 January 2024
Accepted 18 April 2024

To cite: Yang Y, Xu L, Atkins C, *et al*. *Gut* Epub ahead of print: [*please include* Day Month Year]. doi:10.1136/gutjnl-2024-332033

ABSTRACT

Objective Previous studies indicate that eosinophils are recruited into the allograft following orthotopic liver transplantation and protect from ischaemia reperfusion (IR) injury. In the current studies, we aim to explore whether their protective function could outlast during liver repair.

Design Eosinophil-deficient mice and adoptive transfer of bone marrow-derived eosinophils (bmEos) were employed to investigate the effects of eosinophils on tissue repair and regeneration after hepatic IR injury. Aside from exogenous cytokine or neutralising antibody treatments, mechanistic studies made use of a panel of mouse models of eosinophil-specific IL-4/IL-13-deletion, cell-specific IL-4rα-deletion in liver macrophages and hepatocytes and macrophage-specific deletion of heparin-binding epidermal growth factor-like growth factor (hb-egf).

Result We observed that eosinophils persisted over a week following hepatic IR injury. Their peak accumulation coincided with that of hepatocyte proliferation. Functional studies showed that eosinophil deficiency was associated with a dramatic delay in liver repair, which was normalised by the adoptive transfer of bmEos. Mechanistic studies demonstrated that eosinophil-derived IL-4, but not IL-13, was critically involved in the reparative function of these cells. The data further revealed a selective role of macrophage-dependent IL-4 signalling in liver regeneration. Eosinophil-derived IL-4 stimulated macrophages to produce HB-EGF. Moreover, macrophage-specific hb-egf deletion impaired hepatocyte regeneration after IR injury.

Conclusion Together, these studies uncovered an indispensable role of eosinophils in liver repair after acute injury and identified a novel crosstalk between eosinophils and macrophages through the IL-4/HB-EGF axis.

WHAT IS ALREADY KNOWN ON THIS TOPIC

⇒ Eosinophils are rapidly recruited to the liver in response to acute injuries and exert a protective role.
⇒ Recent studies highlighted previously unrecognised functions of eosinophils in resolving inflammation and promoting tissue repair.
⇒ Interleukin (IL)-4 is known to induce alternative activation of macrophages; however, the downstream target involved in macrophage-mediated liver repair is unclear.

WHAT THIS STUDY ADDS

⇒ Demonstrates that eosinophils play an indispensable role in promoting liver repair and regeneration after acute injuries.
⇒ Identifies the selective role of IL-4, but not IL-13, in mediating the reparative function of eosinophils.
⇒ Reveals a novel and essential crosstalk between eosinophils and macrophages, through the IL-4/IL-4Rα/HB-EGF axis, during liver repair and regeneration.

HOW THIS STUDY MIGHT AFFECT RESEARCH, PRACTICE OR POLICY

⇒ Opens up new avenues for research of eosinophil functions in liver pathophysiological conditions.
⇒ Inspires further exploration of eosinophils and/or the IL-4/HB-EGF pathway as therapies to accelerate liver recovery after acute injuries.
⇒ Identifies molecular and cellular targets for the development of strategies to expand donor organ pools for liver transplantation.

INTRODUCTION

Liver transplantation is the only viable treatment for acute liver failure and end-stage chronic liver disease.[1 2] Hepatic ischaemia reperfusion (IR) injury, which occurs during transplantation surgery, is a major factor contributing to acute liver dysfunction and long-term complications, including graft rejection.[3 4] In the USA, there is a significant shortage of donor organs, resulting in approximately 15% yearly mortality of patients waiting for liver transplantation.[5] The increasing demand for liver grafts has led to more frequent use of 'marginal' organs, such as those from older, steatotic and deceased after circulatory death donors.[6] Unfortunately, 'marginal' livers are highly susceptible to IR injury,

resulting in delayed and poor recovery of the grafts.[7 8] Studies of hepatic IR injury have focused mainly on the injury phase.[9–17] There is a critical need to identify molecular and cellular players key to liver repair and regeneration after IR injury.

Eosinophils are a subset of bone marrow-derived granular myeloid cells. The understanding of eosinophil functions has been updated from perceiving them solely as effector cells involved in parasitic infections[18 19] and allergic responses[20–22] to recognising that they are regulators of Local Immunity And/or Remodelling/Repair in both health and disease.[23] Recent emerging studies have highlighted previously unrecognised functions of eosinophils in resolving inflammation and promoting tissue repair. For instance, in acute peritonitis, eosinophils accumulate in the inflamed foci and produce anti-inflammatory and pro-resolving cytokines and lipid mediators.[24 25] In response to cardiotoxin-induced acute skeletal muscle injury, eosinophils rapidly infiltrate the injured tissue and promote fibrogenic/adipogenic progenitor cell proliferation, thereby facilitating muscle regeneration.[26] Another study showed eosinophils play an important role in endometrial stromal cell proliferation, proving crucial in tissue repair after infection.[27] Most recently, three studies demonstrated the essential role of eosinophils in cardiac healing after myocardial infarction.[28–30]

We previously reported that eosinophils were rapidly recruited to the liver following orthotopic liver transplantation in humans and after hepatic IR injury in mice. These cells attenuated injury, through suppressing neutrophils, during the first 24 hours (injury phase) after hepatic IR surgery.[31] Surprisingly, we observed that eosinophils continue to accumulate in the liver beyond the injury phase, with peak accumulation coinciding with the hepatocyte proliferation phase. Using strains of constitutive and inducible eosinophil-deficient mice and an adoptive cell transfer approach, we uncovered an essential role of eosinophils in tissue repair after hepatic IR injury. The data elucidated a novel underlying mechanism involving eosinophil-macrophage crosstalk via an IL-4/HB-EGF-mediated axis.

RESULTS

Eosinophil accumulation in the liver persists during liver repair following hepatic IR injury

Our previous study demonstrated that eosinophils were recruited to the liver within the first 24 hours after hepatic IR injury in mice and exerted a profound protective effect.[31] Surprisingly, when we examined the kinetics of eosinophil accumulation, we observed that these cells persisted in the liver beyond the injury phase. Eosinophils were identified as $CD45^+CD11b^+Ly6G^-SSC^{high}Siglec\text{-}F^+CCR3^+$ cells by flow cytometry. Additionally, immunohistochemical staining was conducted to detect eosinophils using an antibody recognising major basic protein (a generous gift from Dr Elizabeth Jacobsen, Mayo Clinic, Arizona, USA).[32 33] Compared with sham mice, those subjected to IR injury had elevated accumulation of eosinophils in the liver up to 5 days after IR injury, with a peak on day 3 (figure 1A–E), coinciding with the peak of hepatocyte proliferation in wild-type C57Bl/6J (WT) mice (figure 1F,G). These data suggested that eosinophils might contribute to liver repair and regeneration after IR injury.

Eosinophils play an indispensable role in tissue repair after hepatic IR injury

By day 7 after IR injury, the liver nearly completely recovered in WT mice, based on the quantification of necrotic areas and the Suzuki scores (figure 1H–J). To determine the role of eosinophils in liver repair, we used two strains of eosinophil-deficient mice (ΔdblGATA1 and PHIL mice). Compared with WT mice, extensive areas of necrosis (>30% of the liver) remained in both strains on day 7 after IR injury (online supplemental figure S1B–D, F–H). However, one caveat in interpreting the data is that eosinophil-deficient mice had much more severe liver IR injury (online supplemental figure S1A,E), which could contribute to delayed tissue repair. To circumvent this issue, we used inducible eosinophil-deficient (iPHIL) mice, which were generated by knocking-in the human diphtheria toxin (DT) receptor gene into the endogenous eosinophil peroxidase genomic locus.[34] We first established a DT dosing regimen that can achieve eosinophil depletion. The data demonstrated that after two consecutive injections of DT on day 1 and day 2, the number of eosinophils in the blood reduced markedly on day 3 and maintained at low levels of abundance until at least day 8 (online supplemental figure S2A). Based on these results, we administered the first dose of DT to iPHIL mice and WT littermates 16 hours prior to hepatic ischaemia surgery and injected the second dose 6 hours after surgery (figure 2A). This protocol ensured comparable hepatic IR injury between DT-treated WT littermates and iPHIL mice (online supplemental figure S2B) and achieved successful depletion of eosinophils in iPHIL mice after injury and during the time of repair (online supplemental figure S2C,D). We observed a significant delay in tissue repair in iPHIL mice compared with WT littermates, evidenced by larger areas of necrosis and higher Suzuki scores on day 7 after IR surgery (figure 2B–D). These changes coincided with the dramatic reduction of hepatocyte proliferation markers (Ki67 and proliferating cell nuclear antigen (PCNA)) on day 3 (figure 2E–H).

To further investigate the role of eosinophils in liver repair, we adoptively transferred bmEos to eosinophil-deficient mice after IR injury (figure 2I). To evaluate the feasibility, we prepared bmEos from B6-CD45.1 mice and intravenously injected to C57Bl/6J (B6-CD45.2) recipients and tracked the cells by flow cytometry. The data showed rapid infiltration of $CD45.1^+$b-mEos into the recipient's liver within 30 min, reaching its peak at 6 hours postinjection and persisting for at least 3 days post-injection (online supplemental figure S3A,B). After validating the protocol, we adoptively transferred bmEos from WT mice (WT-bmEos) to ΔdblGATA1 and PHIL mice on day 1 after IR surgery. We used this time point to avoid the effects of WT-b-mEos on the extent of injury. As shown in figure 2J–L and online supplemental figure S4A–C, while large areas of necrosis remained after IR surgery in control eosinophil-deficient mice injected with saline, liver histology returned to nearly normal in those that received WT-bmEos. Moreover, hepatocyte proliferation was restored in ΔdblGATA1 mice injected with WT-bmEos (figure 2M–P).

To further validate the pro-repair function of eosinophils, we extended the study to two additional models of acute liver injury caused by acetaminophen (APAP) or carbon tetrachloride (CCl_4). We treated iPHIL mice and their WT littermates with DT 16 hours before and 8 hours after APAP or CCl_4 challenge. As shown in online supplemental figure S5, the WT and iPHIL mice developed similar degrees of liver injury. However, in both acute liver injury models, a significant delay in tissue recovery was observed in iPHIL mice compared with WT littermates. This was evidenced by the presence of larger areas of necrosis and higher Suzuki scores on day 6 after APAP or CCl_4 treatment. Together, these data provide strong evidence that eosinophils play an essential role in the liver repair process after acute injury.

To understand how eosinophils promote liver repair after IR injury, we performed a cytokine array analysis (Proteome Profiler

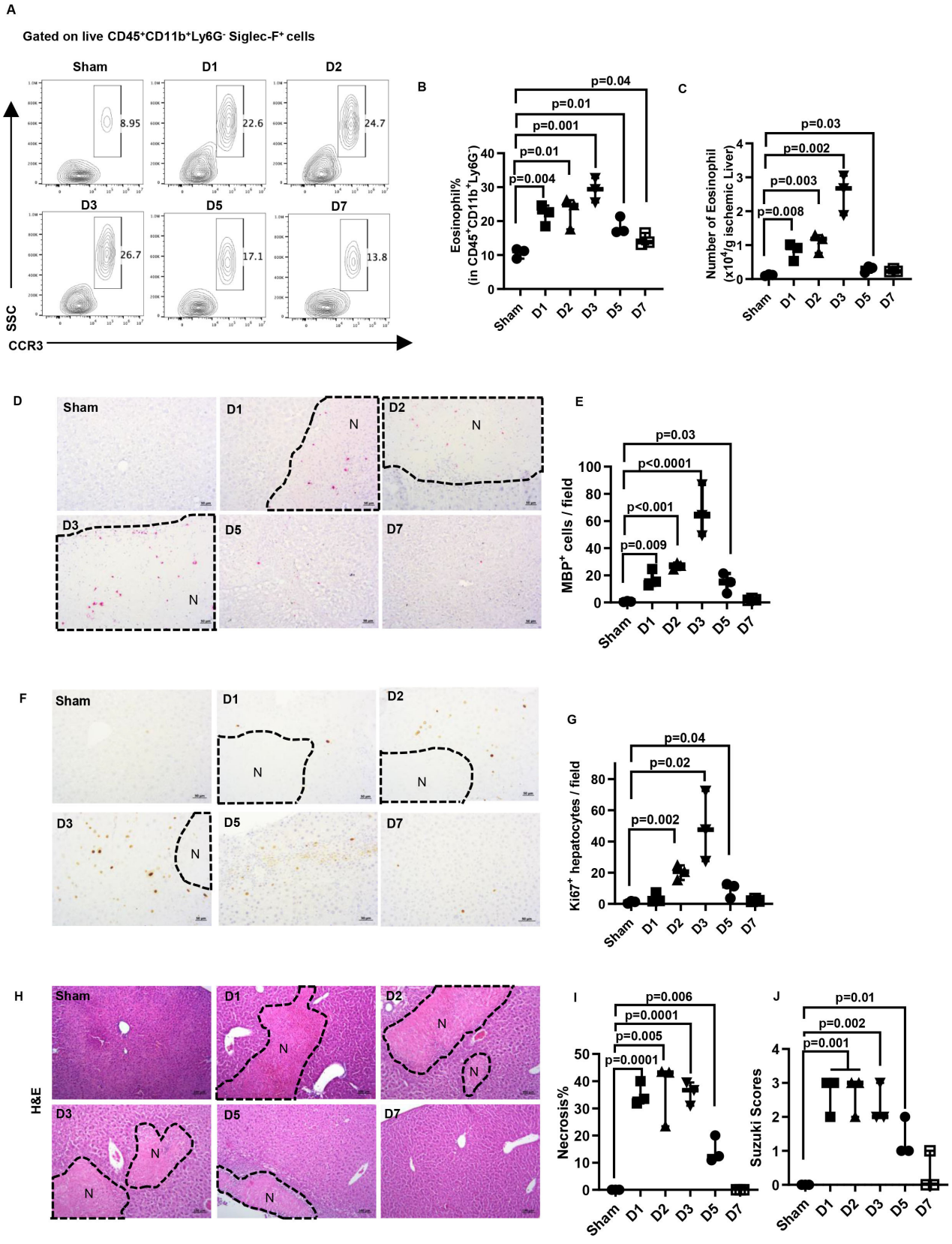

Figure 1 The kinetics of hepatic eosinophil accumulation and the time course of liver repair after IR injury in WT mice. Male C57Bl/6J mice were subjected to hepatic ischemia (60 mins) followed by reperfusion and sacrificed at various times (n=3/group). Sham mice underwent the same surgery without vascular blockage and were sacrificed on day 7. (A-C) The percentage and numbers of eosinophils ($CD45^+CD11b^+Ly6G^-Siglec\text{-}F^+CCR3^+$cells) in the liver were measured by flow cytometry and quantified. (D, E) IHC staining for eosinophils by anti-mouse major basic protein (MBP) antibody and the numbers of MBP^+ cells quantified. (F, G) Proliferating hepatocytes were stained by anti-Ki67 antibody, and the numbers of positive cells were quantified. (H, I) Liver necrosis (N, outlined areas) was evaluated and quantified. (J) Liver pathology was assessed by using the Suzuki's scoring system. Two-tailed unpaired Student's t-test with Welch's correction was performed in B, C, E, G, I and J.

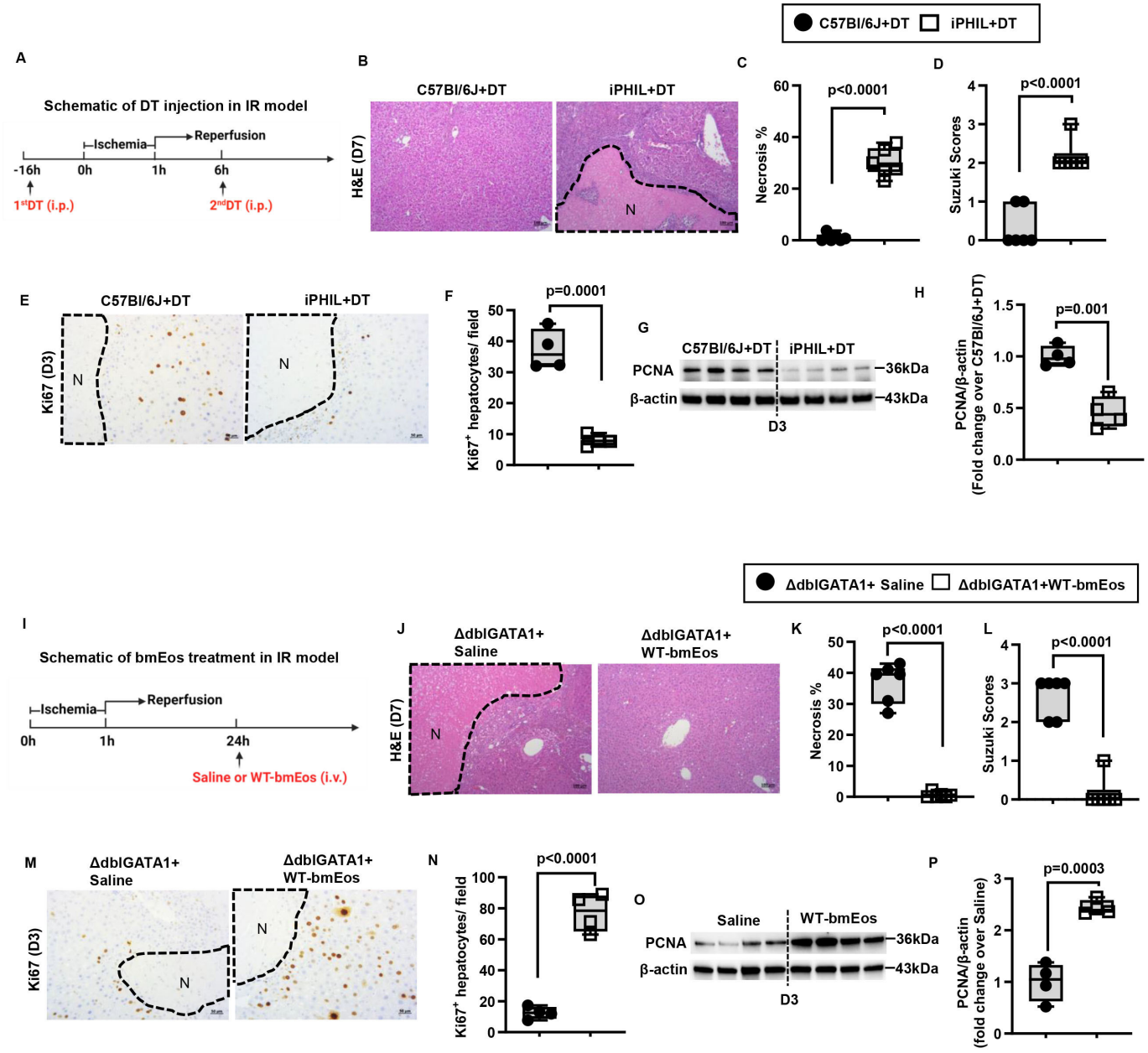

Figure 2 Eosinophils promote liver repair after IR injury. (A-H) Male iPHIL mice and WT littermates were subjected to hepatic IR surgery. Mice were administered (i.p.) the first dose of DT at 16h prior to IR surgery and the second dose at 6h after surgery. Mice were sacrificed on day 3 (n=4/group) or day 7 (n=6/group) after IR surgery. (B, C) Liver necrosis (N, outlined areas) was evaluated and quantified on day 7 after IR surgery. (D) Liver pathology was determined by the Suzuki score on day 7 after IR surgery. (E, F) Liver tissue sections were stained for Ki67 to quantify proliferating hepatocytes on day 3 after IR surgery. (G, H) PCNA protein expression was detected by Western blotting and quantified. (I-P) Male ΔdblGATA-1 mice were subjected to hepatic IR surgery. After 24h, half of the mice were i.v. injected with bmEos ($10x10^6$) and the other half injected with saline as control. Mice were sacrificed on day 3 (n=4/group) or day 7 after IR surgery (n=6/group). (J, K) Liver necrosis (N, outlined area) was evaluated and quantified on day 7 after IR surgery. (L) Liver pathology was determined by the Suzuki score on day 7 after IR surgery. (M, N) Proliferative hepatocytes were stained for Ki67 and quantified on day 3 after IR surgery. (O, P) PCNA protein expression was detected by Western blotting and quantified. Two-tailed unpaired Student's t-test with Welch's correction was performed in C, D, F, H, K, L, N and P.

Mouse Cytokine Array Kit). The data demonstrated IL-4 and IL-13 as the most significantly upregulated cytokines on adoptive transfer of WT-bmEos to ΔdblGATA1 mice (online supplemental figure S6). To further investigate the cellular source of IL-4 and IL-13, we performed flow cytometric analyses using IL-4/GFP-enhanced transcript (4Get) mice to measure IL-4 expression and intracellular staining to detect IL-13. The data showed that eosinophils accounted for >86% of IL-4-positive cells and >90% of IL-13-positive cells in the liver (online supplemental figure S7A,B), suggesting that IL-4 and IL-13 are mainly produced by eosinophils during tissue repair. To investigate the role of eosinophil-derived IL-4 and/or IL-13 in liver repair, we generated mice with eosinophil-specific deletion of both IL-4 and IL-13 (Il-4/13$^{fl/fl}$eoCre$^{+/-}$). We obtained bmEos from these mice and their WT littermates (Il-4/13$^{fl/fl}$eoCre$^{-/-}$) and adoptively transferred the cells to ΔdblGATA1 mice on day 1 after hepatic IR injury (figure 3A). While WT-bmEos restored liver repair in ΔdblGATA1 mice, IL-4/13-deleted bmEos failed

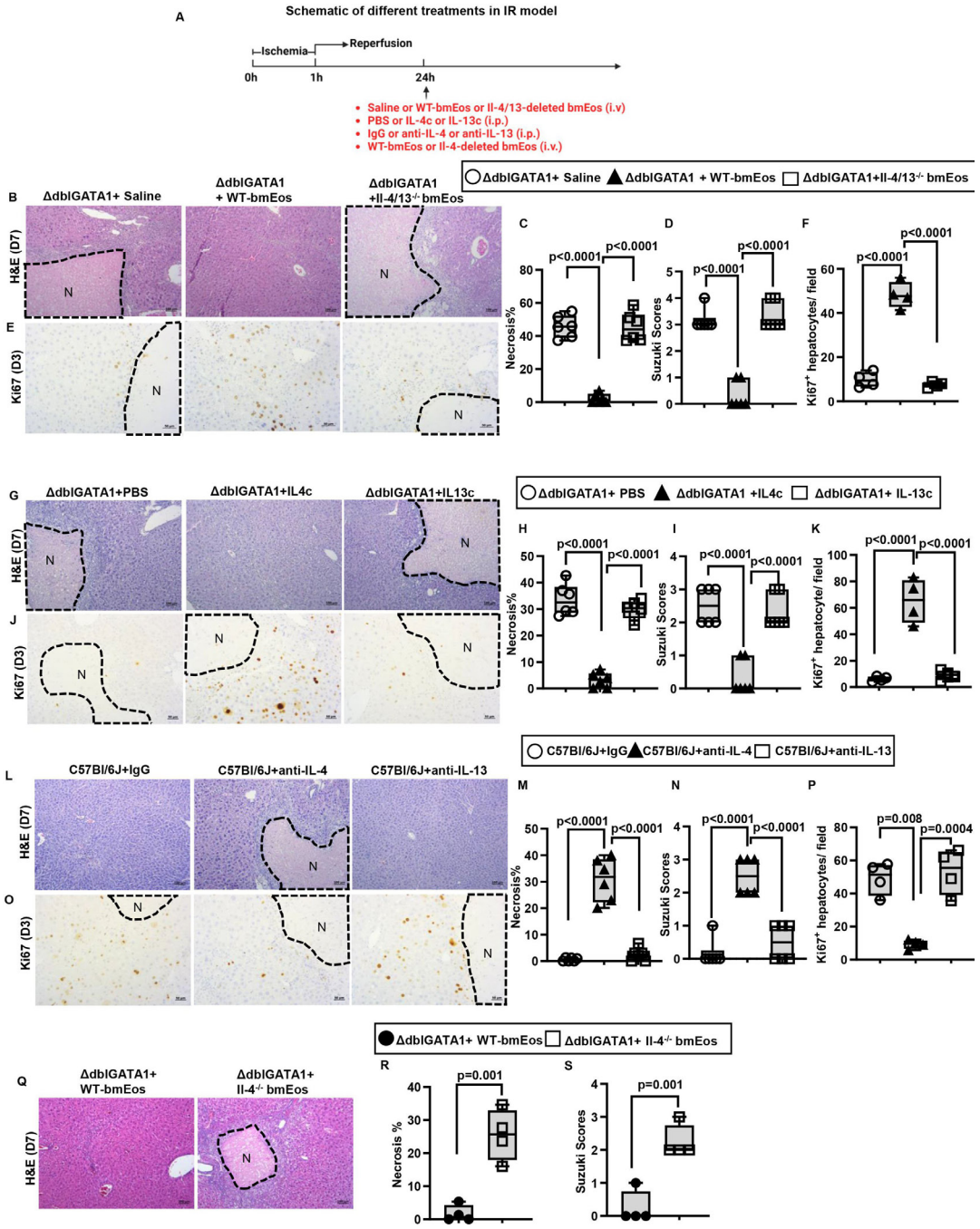

Figure 3 Eosinophil-derived IL-4 plays a critical role in liver repair after IR injury. (A-F) Male ΔdblGATA-1 were subjected to hepatic IR surgery. After 24h, the mice were divided into three groups and i.v. injected with saline, WT-bmEos ($10x10^6$) or Il-4/13-deleted bmEos ($10x10^6$). Mice were sacrificed on day 3 (n=4/group) or day 7 (n=6/group) after IR surgery. (B, C) Liver necrosis (N, outlined areas) was evaluated and quantified on day 7 after IR surgery. (D) Liver pathology was assessed by using the Suzuki's scoring system on day 7 after IR surgery. (E, F) Proliferative hepatocytes were stained for Ki67 and quantified on day 3 after IR surgery. (A, G-K) Male ΔdblGATA-1 were subjected to hepatic IR surgery. After 24h, the mice were divided into three groups and i.p. injected with PBS, IL-4c (5 μg recombinant IL-4 complexed to 25 μg anti-IL-4 antibody) or IL-13c (5 μg of recombinant IL-13 complexed to 25 μg anti-IL-13 antibody). Mice were sacrificed on day 3 (n=4/group) or day 7 (n=6/group). (G, H) Liver necrosis (N, outlined areas) was evaluated and quantified on day 7 after IR surgery. (I) Liver pathology was assessed by using the Suzuki's scoring system quantified on day 7 after IR surgery. (J, K) Proliferative hepatocytes were stained for Ki67 and quantified on day 3. (A, L-P) Male C57Bl/6J mice were subjected to hepatic IR surgery. On day 1 and day 3 after surgery, the mice were i.p. injected with anti-IL-4 antibody (10 μg/mouse) or anti-IL-13 antibody (10 μg/mouse). Control mice were injected with IgG. Mice were sacrificed on day 3 (n=4/group) or day 7 (n=6/group) after IR surgery. (L, M) Liver necrosis (N, outlined areas) was evaluated and quantified on day 7 after IR surgery. (N) Liver pathology was assessed by using the Suzuki's scoring system on day 7 after IR surgery. (O, P) Proliferative hepatocytes were stained for Ki67 and quantified on day 3. (A, Q-S) Male ΔdblGATA-1 mice were subjected to hepatic IR surgery. After 24h, half of the mice were i.v. injected with WT-bmEos ($10x10^6$) and the other half injected with Il-4-deleted bmEos ($10x10^6$). Mice were sacrificed on day 7 after IR surgery (n=4/group). (Q, R) Liver necrosis (N, outlined areas) was evaluated and quantified on day 7 after IR surgery. (S) Liver pathology was assessed by using the Suzuki's scoring system on day 7 after IR surgery. Two-tailed unpaired Student's t-test with Welch's correction was performed in R and S. One-way ANOVA was performed in C, D, F, H, I, K, M, N and P.

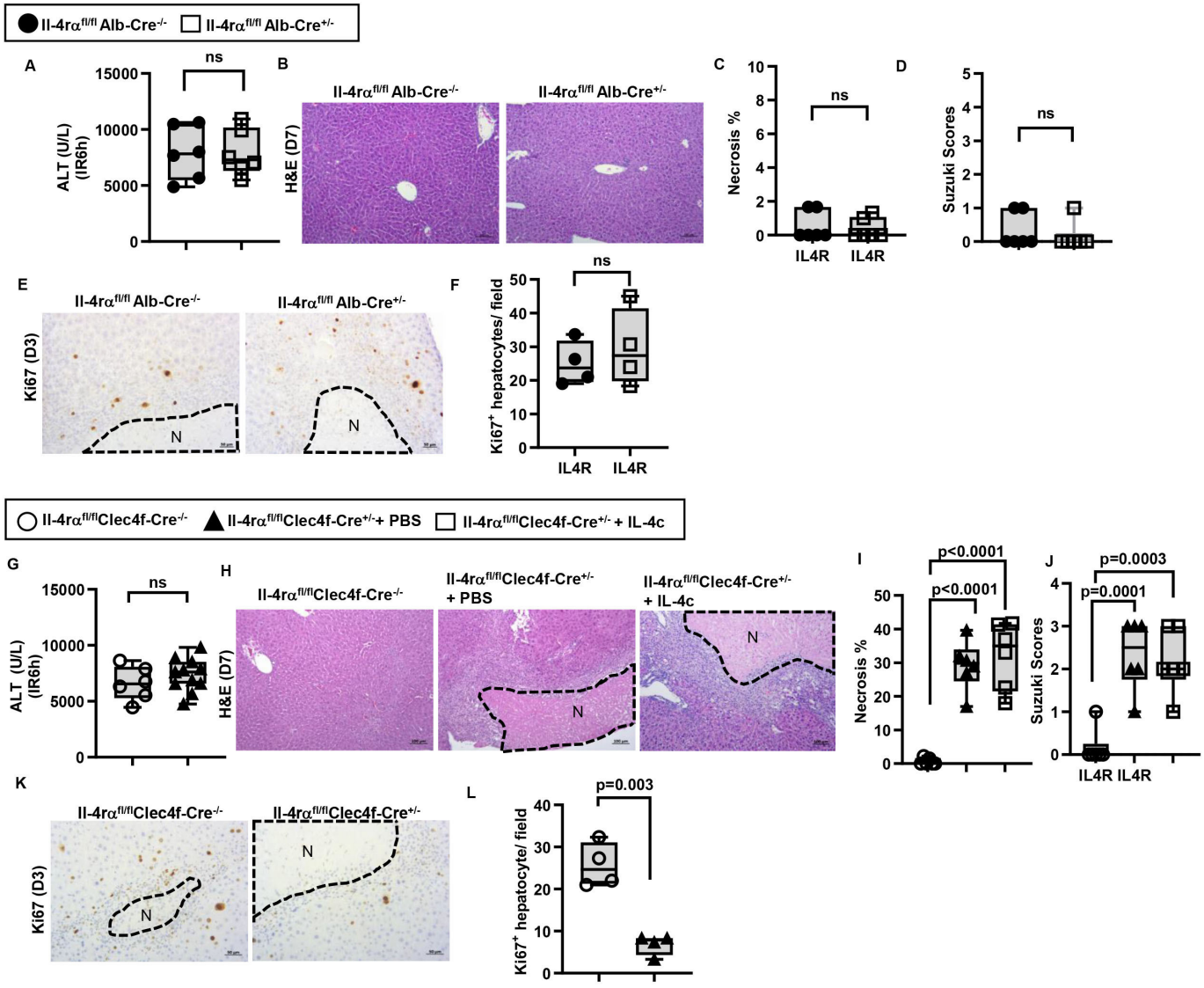

Figure 4 IL-4Rα signaling in liver macrophages, rather than hepatocytes, promotes liver repair after IR injury. (A-F) Male Il-4rα$^{fl/fl}$Alb-Cre$^{+/-}$ mice and WT littermates (Male Il-4rα$^{fl/fl}$Alb-Cre$^{-/-}$) were subjected to hepatic IR surgery and sacrificed after 3 days (n=4/group) or 7 days (n=6/group). (G-L) Male Il-4rα $^{fl/fl}$Clec4f-Cre$^{+/-}$ mice and WT littermates (Il-4rα$^{fl/fl}$Clec4f-Cre$^{-/-}$) were subjected to hepatic IR surgery. After 24h, the Il-4rα$^{fl/fl}$Clec4f-Cre$^{+/-}$ mice were divided into two groups and injected (i.v.) with PBS or IL-4c (n=6/group) and and sacrificed after 3 days (n=4/group) or 7 days (n=6/group) after IR surgery. (A, G) Serum ALT levels 6h after IR surgery. (B, C, H, I) Liver necrosis (N, outlined areas) was evaluated and quantified on day 7 after IR surgery. (D, J) Liver pathology was assessed by using the Suzuki's scoring system on day 7 after IR surgery. (E, F, K, L) Proliferative hepatocytes were stained for Ki67 and quantified on day 3 after IR surgery. Two-tailed unpaired Student's t-test with Welch's correction was performed in A, C, D, F, G and L. One-way ANOVA was performed in I and J.

to improve liver repair compared with control ΔdblGATA1 mice injected with saline (figure 3B–D). Congruent with this observation, the adoptive transfer of WT-bmEos, but not IL-4/13-deleted bmEos, significantly increased hepatocyte proliferation in ΔdblGATA1 mice on day 3 after IR injury (figure 3E,F). These data suggest that eosinophil-derived IL-4 and/or IL-13 are critically involved in liver repair and regeneration after IR injury.

Eosinophils promote liver tissue repair through IL-4 production

To further determine whether the delayed liver repair in ΔdblGATA1 mice was due to the lack of eosinophil-derived IL-4 or IL-13, we injected IL-4/anti-IL-4 mAb complex (IL-4c) or IL-13/anti-IL-13 mAb complex (IL-13c) to ΔdblGATA1 mice (figure 3A). We used the antibody-conjugated cytokines to prolong the half-life of the cytokines as reported in many studies.[35–38] Our data showed that IL-4c injection could significantly increase hepatocyte proliferation (figure 3J,K) and accelerate liver repair (figure 3G–I). Moreover, blockade of IL-4 by a neutralising antibody significantly delayed liver repair in WT mice, as demonstrated by decreased numbers of Ki67$^+$ hepatocytes on day 3 after IR injury as well as increased Suzuki scores and extents of live necrosis on day 7 (figure 3L–P). In contrast, we did not observe any improvement of liver repair in ΔdblGATA1 mice treated with IL-13c, nor any inhibitory effect by IL-13 blockade on liver repair in WT mice (figure 3G–P). To further corroborate these results, we adoptively transferred bmEos obtained from IL-4$^{-/-}$ mice to ΔdblGATA-1 mice on day 1 after IR surgery (figure 3A). Our data showed that IL-4-deleted bmEos, although expressing IL-13, could not restore liver repair in ΔdblGATA1 mice (figure 3Q–S). Taken together, these data strongly suggest that eosinophil-derived IL-4,

Table 1 Proliferation-related proteins expression in the liver tissues from mice with hepatic macrophages-specific IL-4Rα deletion

Protein name	Il-4rα$^{fl/fl}$Clec4f-Cre$^{-/-}$ Average of protein expression level±SEM	Il-4rα$^{fl/fl}$Clec4f-Cre$^{+/-}$ Average of protein expression level±SEM	Fold difference±SEM (Il-4rα$^{fl/fl}$Clec4f-Cre$^{+/-}$ vs Clec4f-Cre$^{-/-}$)
EGFR_pY1173	0.95±0.03	0.71±0.09	0.73±0.07
Stat3_pY705	1.04±0.09	1.13±0.12	1.08±0.02
MAPK_pT202_Y204	0.84±0.16	1.17±0.32	1.35±0.14
b-Catenin_pT41_S45	1.02±0.07	0.93±0.06	0.91±0.02
Akt_pS473	1.09±0.15	1.03±0.12	0.96±0.06
Akt_pT308	1.02±0.02	0.96±0.08	0.94±0.09
Akt1_pS473	1.06±0.16	1.13±0.13	1.08±0.06
mTOR_pS2448	1.03±0.06	0.87±0.03	0.85±0.04
c-Met_pY1234_Y1235	1.04±0.05	1.01±0.06	0.97±0.03
BMK1-Erk5_pT218_Y220	1.1±0.2	1.12±0.19	1.03±0.03

Il, interleukin.

but not IL-13, plays a critical role in promoting liver regeneration and repair after IR injury.

IL-4Rα signalling in hepatic macrophage orchestrates liver repair after IR injury

The direct effect of IL-4 on hepatocytes has been investigated in the context of liver regeneration after non-injurious partial hepatectomy, but the results are controversial. One study suggested that IL-4 could stimulate hepatocyte proliferation[39]; however, another study showed that IL-4 did not directly affect hepatocyte proliferation.[40] To investigate if hepatocytes are a direct target of IL-4, we generated a mouse line with hepatocyte-specific IL-4rα-deletion (Il-4rα$^{fl/fl}$Alb-Cre$^{+/-}$). After IR surgery, these mice showed similar degrees of liver injury with no effect on tissue recovery (figure 4A–F). These data ruled out a direct effect of IL-4 on hepatocytes during liver regeneration and repair after IR injury.

To search for IL-4 target cells, we screened for IL-4Rα expression in NPCs. Our data showed that >70% of IL-4Rα-positive cells were macrophages (F4/80^{+}), and the rest were liver sinusoidal endothelial cells (CD31^{+}) (online supplemental figure S8). To further address whether IL-4 promotes liver repair through IL-4Rα signalling in macrophages, we generated macrophage-specific Il-4rα-deleted mice using Clec4f-Cre mice, which have been used to successfully generate liver macrophage-specific gene knockout mice.[41–43] We subjected Il-4rα$^{fl/fl}$Clec4f-Cre$^{+/-}$ mice and WT littermates (Il-4rα$^{fl/fl}$Clec4f-Cre$^{-/-}$) to hepatic IR surgery and observed similar degrees of liver injury (figure 4G). However, liver regeneration was significantly delayed in the Il-4rα$^{fl/fl}$Clec4f-Cre$^{+/-}$ mice, evidenced by larger areas of necrosis, higher Suzuki scores and lower numbers of Ki67^{+} hepatocytes than WT littermates (figure 4H–L). Interestingly, treatment of Il-4rα$^{fl/fl}$Clec4f-Cre$^{+/-}$ mice with IL-4c did not improve liver repair (figure 4H–J), despite the presence of intact IL-4Rα on other cells. Taken together, these data demonstrate that the pro-repair effects of IL-4 after IR injury are mediated through IL-4Rα signalling in hepatic macrophages.

IL-4-induced HB-EGF production by hepatic macrophages plays an essential role in liver repair after IR injury

To further understand how IL-4/IL-4Rα signalling in hepatic macrophages contributes to tissue repair and regeneration after IR injury, we performed a Reverse Phase Protein Array (RPPA) experiment using liver samples harvested on day 3 after IR injury. The data revealed a reduced level of phosphorylated(p)-epidermal growth factor receptor (p-EGFR) in the liver of Il-4rα$^{fl/fl}$Clec4f-Cre$^{+/-}$ mice compared with WT littermates (table 1). This result was confirmed by western blot analyses (figure 5A,B), and suggested that the IL-4/IL-4Rα signalling in hepatic macrophages could regulate one or more EGFR ligands. Thus, we purified hepatic macrophages from Il-4rα$^{fl/fl}$Clec4f-Cre$^{+/-}$ mice and WT littermates on day 3 after IR injury and measured mRNA levels of all seven known EGFR ligands, including Egf, transforming growth factor alpha, Hb-egf, amphiregulin, epigen, epiregulin and betacellulin. The data showed that only the expression of Hb-egf was reduced in hepatic macrophages from Il-4rα$^{fl/fl}$Clec4f-Cre$^{+/-}$ mice (figure 5C). To determine if IL-4, through IL-4Rα, directly triggers macrophages to produce HB-EGF, we treated bone marrow-derived macrophages (BMDM) from WT and Il-4rα$^{-/-}$ mice with IL-4. The data showed that IL-4 dramatically upregulated hb-egf mRNA and protein levels in WT-BMDM, but not in IL-4rα-deleted BMDM (figure 5D,E). Given our data showing that liver sinusoidal endothelial cell (LSEC) also express IL-4Rα (online supplemental figure S8), we isolated LSECs from naïve mice and treated them with IL-4. Interestingly, IL-4 did not induce hb-egf expression in LSECs (online supplemental figure S9), suggesting that IL-4/IL-4Rα-mediated signalling in LSECs does not significantly contribute to HB-EGF production. Taken together, these results suggest that (1) hepatic macrophages represent the predominant source of HB-EGF during liver IR injury and (2) the IL-4/IL-4Rα signalling is critical in HB-EGF production by macrophages.

Male Il-4rα$^{fl/fl}$Clec4f-Cre$^{+/-}$ mice and WT littermates (male Il-4rα$^{fl/fl}$Clec4f-Cre$^{-/-}$) were subjected to hepatic IR surgery and sacrificed after 3 days. Liver tissue samples were processed and used for the RPPA screening.

To investigate the involvement of HB-EGF in tissue repair after IR injury, we injected recombinant mouse HB-EGF into Il-4rα$^{fl/fl}$Clec4f-Cre$^{+/-}$ mice on days 1 and 3 after IR injury. As shown in figure 5F–H, exogenous HB-EGF restored liver repair by day 7 in these mice. To further determine whether HB-EGF produced by hepatic macrophages, rather than other cells, plays a critical role in liver repair, we generated a mouse with hepatic macrophage-specific deletion of hb-egf (Hb-egf$^{fl/fl}$Clec4f-Cre$^{+/-}$). Figure 6A shows that these mice developed similar degrees of liver injury compared with WT littermates after IR surgery. However, whereas WT mice recovered by day 7 after IR injury, Hb-egf$^{fl/fl}$Clec4f-Cre$^{+/-}$ mice continued to show extensive areas of necrosis (>35% of the liver) with higher Suzuki scores (figure 6B–D). In line with this observation, hepatocyte proliferation, as quantified by Ki67 staining and hepatic PCNA expression, was also dramatically decreased in Hb-egf$^{fl/fl}$Clec4f-Cre$^{+/-}$ mice on day 3 after IR injury (figure 6E–H).

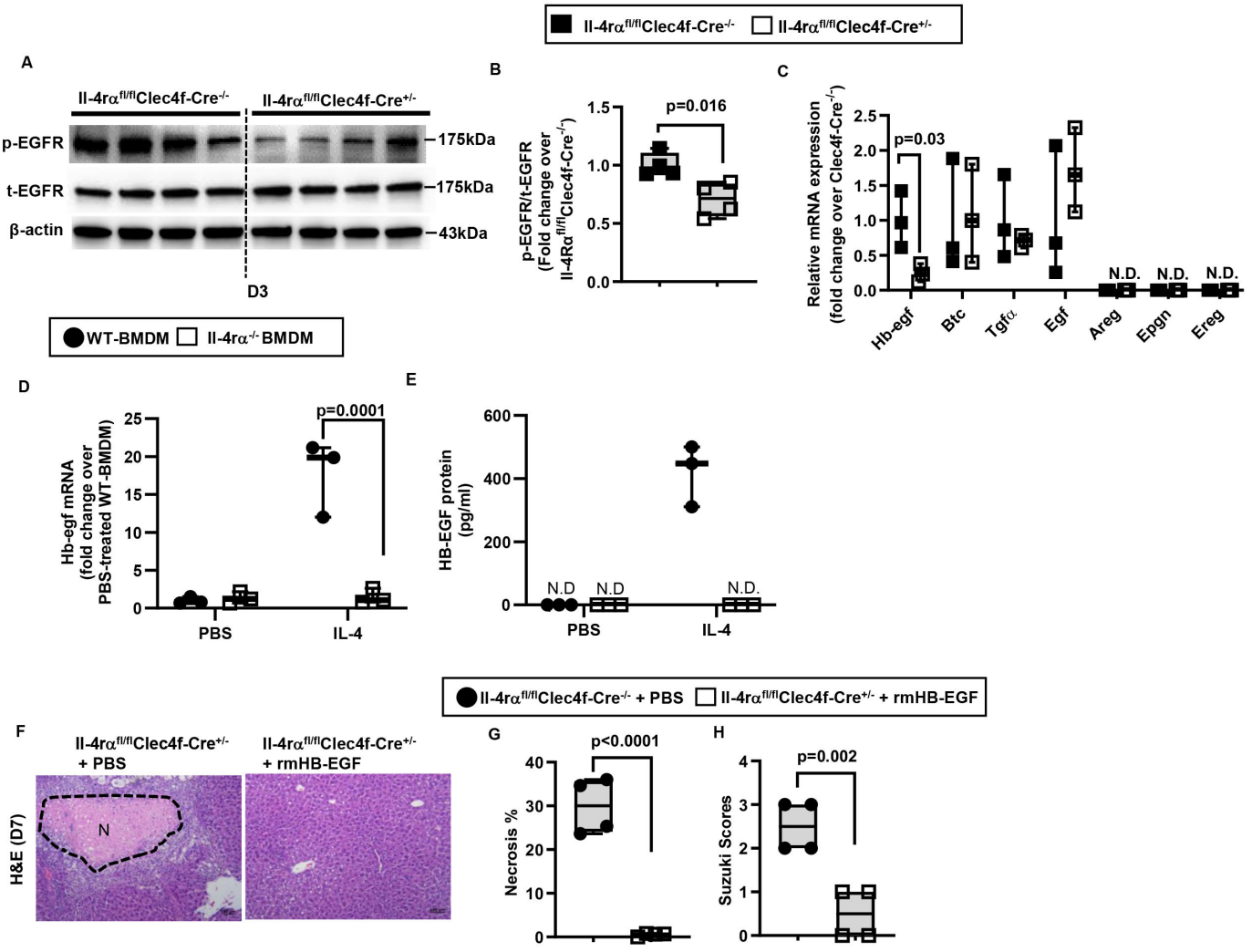

Figure 5 IL-4/IL-4Rα signaling in hepatic macrophage induces HB-EGF expression. (A-C) Male Il-4rα$^{fl/fl}$Clec4f-Cre$^{+/-}$ mice and WT littermates (Male Il-4rα$^{fl/fl}$Clec4f-Cre$^{-/-}$) were subjected to hepatic IR surgery and sacrificed after 3 days. Liver tissues were collected and hepatic macrophages were purified by magnetic-associated cell sorting (MACS) using anti-F4/80 antibody. (A, B) phospho(p)-EGFR and total (t)-EGFR protein levels in the liver tissue were detected by Western blotting and quantified (n=4/group). (C) mRNA levels of all EGFR ligands expressed by hepatic macrophages were measured by q-PCR (n=3/group). (D, E) WT-BMDM and Il-4rα-deleted BMDM were cultured with IL-4 for 6h or 24h. Control groups were treated with PBS (n=3/group). mRNA and protein levels of HB-EGF were measured at 6h by q-PCR and 24h by ELISA, respectively. (F-H) rmHB-EGF was i.p. injected to male Il-4rα$^{fl/fl}$Clec4f-Cre$^{+/-}$ mice on day 1 and day 3 after liver IR surgery. Control mice were injected with PBS. All mice were sacrificed on day 7 after IR surgery (n=4/group). (F, G) Liver necrosis (N, outlined areas) was evaluated and quantified on day 7. (H) Liver pathology was assessed by using the Suzuki's scoring system. Two-tailed unpaired Student's t-test with Welch's correction was performed in B, C, G and H. One-way ANOVA was performed in D and E.

In addition, western blot analyses showed that the p-EGFR levels were significantly lower in Hb-egf$^{fl/fl}$Clec4f-Cre$^{+/-}$ mice than WT littermates (figure 6I–J). Moreover, treatment of Hb-egf$^{fl/fl}$Clec4f-Cre$^{+/-}$ mice with IL-4c could not restore liver repair after IR injury (figure 6B–D), suggesting that the pro-repair function of IL-4 is dependent on hepatic macrophage-derived HB-EGF. Collectively, these data demonstrate that IL-4/IL-4Rα signalling in hepatic macrophages results in HB-EGF production which is essential in liver regeneration and repair after IR injury.

Discussion

The current studies demonstrate that eosinophils, persisting in the liver beyond the injury phase, orchestrate liver repair after IR injury and acute injury caused by APAP and CCl_4. Eosinophil-derived IL-4, but not IL-13, activates hepatic macrophages through IL-4Rα signalling to produce HB-EGF, thereby facilitating hepatocyte proliferation.

Tissue repair after injury is a complex process critical for the survival of the organism. Subsets of innate immune cells are recruited to the wound site to clear debris and dead cells,[44–46] triggering the proliferation of epithelial cells or progenitor cells[47–50] and inducing vascularisation.[51] The involvement of eosinophils in tissue repair has emerged as a previously unrecognised function. Recent studies of skeletal muscle injury, peritonitis and myocardial infarction have demonstrated the indispensable role of these cells in tissue repair.[24–26 28–30 52] Our current study, using congenic and iPHIL mice and adoptive transfer of bmEos, provides the first evidence to support the indispensable role of eosinophils in liver repair after IR injury and in other models of acute liver injury, caused by APAP and CCl_4. An observation common in the published studies and ours is

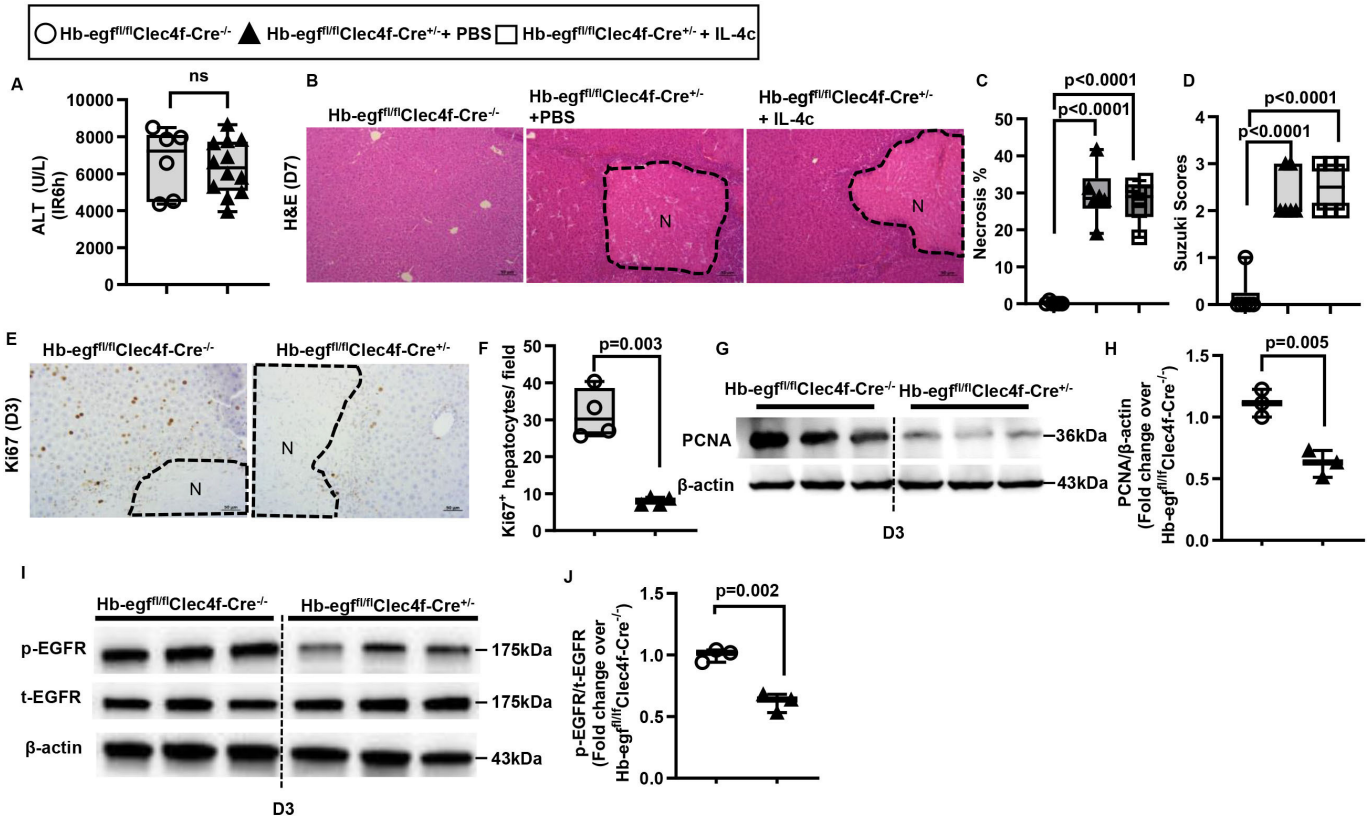

Figure 6 Liver repair after IR injury is impaired when hb-egf is deleted in hepatic macrophages. Male Hb-egf$^{fl/fl}$Clec4f-Cre$^{+/-}$mice and WT littermates (Male Hb-egf$^{fl/fl}$Clec4f-Cre$^{-/-}$) were subjected to hepatic IR surgery. After 24h, Hb-egf$^{fl/fl}$Clec4f-Cre$^{+/-}$ mice were divided into two groups and injected (i.p.) with PBS or IL-4c (n=6/group). (A) Serum ALT levels at 6h after IR surgery. (B, C) Liver necrosis (N, outlined areas) was evaluated and quantified on day 7 after IR surgery. (D) Liver pathology was assessed by using the Suzuki's scoring system on day 7 after IR surgery. (E, F) Proliferative hepatocytes were stained for Ki67 and quantified on day 3 after IR surgery (n=4/group). (G, H) PCNA protein expression was detected by Western blotting and quantified. (I, J) p-EGFR and t-EGFR protein expression levels were detected by Western blotting and quantified. Two-tailed unpaired Student's t-test with Welch's correction was performed in A, F, H and J. One-way ANOVA was performed in C and D.

that structural cell damage results in eosinophil infiltration to the injured tissues.[31 53] This is probably because that injured tissues compel macrophages to release eotaxin-2 (CCL24), a crucial eosinophil chemoattractant,[53] and type 2 innate lymphoid cells (ILC2s) are suggested to be potent inducers of eosinophil migration, either through their production of IL-5 or potentially through the production of eotaxin-1 (CCL11).[54–56] In contrast, when cellular injury does not occur, such as in partial hepatectomy (PHx), we did not observe eosinophil infiltration to the liver (data not shown). However, there is one report describing that eosinophil-derived IL-4 could promote hepatocyte proliferation after PHx.[39] Given that PHx causes intestinal perturbation, it is possible that eosinophils, which are abundant in the gut, may contribute to liver regeneration. The notion that IL-4 can directly stimulate hepatocyte proliferation is contradicted by another study of PHx,[40] which showed that IL-4 did not directly affect hepatocyte proliferation. We generated mice with hepatocyte-specific IL-4Rα deletion to investigate if hepatocytes were a direct cellular target of IL-4. Our data ruled out this possibility and instead demonstrated that hepatocyte proliferation was attenuated when IL-4Rα was deleted in hepatic macrophages.

Macrophages are critically involved in the tissue repair process. A recent study of concanavalin A-induced acute liver injury demonstrated that hepatic macrophages encircled the necrotic areas to prevent further damage of hepatocytes and eventually eliminate necrotic lesions.[57] It is known that macrophages adopt an inflammatory phenotype when they first enter an injured or infected tissue. They then switch to a pro-repair phenotype with the production of anti-inflammatory cytokines, growth factors and angiogenic factors.[58–60] Although it is widely considered that macrophage activation through IL-4Rα contributes to tissue repair, the experimental evidence had been circumstantial. In vivo studies of macrophage-specific deficiency of IL-4Rα or identifying macrophage-derived pro-repair molecules are lacking. The current study filled a knowledge gap regarding how macrophage plasticity is regulated. Our data demonstrate that eosinophils play a crucial role, through IL-4, in promoting macrophages to produce HB-EGF that is necessary for liver repair after IR injury.

With regard to activating macrophages, IL-4 and IL-13 have been considered indistinguishable in promoting M2 polarisation.[38 61 62] However, a more detailed investigation of downstream effects revealed differential gene targeting by IL-4 vs IL-13. Our data demonstrate that IL-4, but not IL-13, triggers HB-EGF production by macrophages. We also found that IL-4, but not IL-13 could rescue liver repair in ΔdblGATA1 mice. Antibody-mediated neutralisation of IL-4, but not IL-13, significantly delayed liver repair after IR injury in WT mice. Although IL-4 and IL-13 share the same receptor, IL-4Rα/IL-13Rα1, IL-4 is known to also bind to IL-4Rα/γc, which may contribute to the unique functions of IL-4. In congruent with our finding, several studies of tissue repair after myocardial infarction show the involvement of IL-4, but not IL-13.[28–30] Another

study of traumatic muscle wounds also showed that implantation of biomaterial scaffold induced a pro-regenerative response mediated by T helper 2 activation to produce IL-4.[63]

Through binding to EGF receptors, HB-EGF promotes cell proliferation, migration, adhesion and differentiation.[64] Owing to these functions, HB-EGF has been implicated in wound healing and repair after injury in many tissues.[65] In the liver during recovery from injuries, the level of HB-EGF is elevated.[66] Studies of liver injury caused by CCl_4, activation of Fas receptor or bile duct ligation show that HB-EGF treatment increases hepatocyte proliferation, decreases cell death and reduces areas of fibrosis.[67–69] The current study provides the first evidence that HB-EGF plays a critical role in promoting liver repair after IR injury. More importantly, our data demonstrate that liver repair is significantly delayed when HB-EGF is specifically deleted from hepatic macrophages, suggesting that macrophages are a major source of HB-EGF. This is consistent with the fact that HB-EGF was first identified in the culture medium of human peripheral blood mononuclear cells.[70] Further studies suggested that M2 polarised macrophages were a source of HB-EGF. For example, a head and neck cancer cell line (CAL17) co-cultured with M2 macrophages was resistant to radiation in an HB-EGF-dependent manner.[71] Another in vitro study showed that co-culture with M2-polarised macrophages increased ovarian cancer cell proliferation and that this effect was abrogated by HB-EGF neutralising antibodies.[72] A more recent in vivo study demonstrated that macrophages that infiltrated into the pancreas after cerulein-induced experimental pancreatitis produced high levels of HB-EGF. Importantly, this study showed that myeloid-specific HB-EGF deletion impaired DNA repair and decreased epithelial cell proliferation, resulting in delayed tissue recovery after pancreatic injury.[73] It is known that HB-EGF is synthesised as a membrane-bound pro-HB-EGF, which is cleaved by a disintegrin and metalloprotease (ADAM) and matrix metalloproteinase, and the pro-inflammatory cytokine IL-1β to soluble HB-EGF.[74 75] Although both pro-HB-EGF and soluble-HB-EGF can bind to the EGF receptor,[65 76] a limitation of the current study is that we have yet to elucidate which form is at play. It may be possible that the IL-4/IL-4Rα signalling in macrophages is important in promoting HB-EGF synthesis and is involved in the shedding of pro-HB-EGF.

Another limitation of this study is the primary focus on hepatocyte proliferation during the liver repair process. It is important to recognise that the eosinophil-macrophage crosstalk may also impact other aspects of liver repair, such as resolving inflammation, remodelling extracellular matrix and promoting angiogenesis. These possibilities warrant further investigation in order to gain a better understanding of the pro-repair function of eosinophils.

In summary, we uncovered a previously unappreciated pro-repair function of eosinophils after hepatic IR injury. The experimental findings provided insights into the underlying mechanism of liver repair involving eosinophil and macrophage crosstalk through IL-4 signalling and HB-EGF production. There is currently no treatment modality to improve or accelerate tissue recovery after hepatic IR injury. Developing such a modality could enable the safe transplantation of 'marginal' livers and expand the donor organ pools. The current study provides strong evidence to further explore eosinophils and the IL-4/HB-EGF axis as novel approaches to improve the outcomes of liver transplantation and patients with acute liver injury.

Author affiliations
[1]Department of Anesthesiology, Critical Care and Pain Medicine, McGovern Medical School, University of Texas Health Science Center at Houston, Houston, TX, USA
[2]The University of Texas Health Science Center at Houston, Houston, TX, USA
[3]Department of Surgery, McGovern Medical School, University of Texas Health Science Center at Houston, Houston, TX, USA
[4]Laboratory of Liver Disease, National Institute on Alcohol Abuse and Alcoholism, NIH, Bethesda, MD, USA
[5]University of Cape Town Faculty of Health Sciences, Observatory, Western Cape, South Africa
[6]Division of Nephrology and Hypertension, Department of Medicine, Vanderbilt University School of Medicine, Nashville, TN, USA
[7]Division of Allergy, Asthma and Clinical Immunology, Mayo Clinic Arizona, Scottsdale, AZ, USA

Contributors YY designed and performed mouse experiments and various analyses. LX performed mouse experiments and flow cytometric analyses. YY prepared the figures and the manuscript. CA and LK performed immunohistochemical analyses. JZ, J-MJ, YW, NM, KHK, YAA, FW, SB, VV, BG and HKE reviewed and revised the manuscript. FB, RH and EJ generated and provided essential transgenic mouse lines. CJ conceptualised and supervised the study and revised the manuscript. CJ is the author responsible for the overall content as the guarantor.

Competing interests None declared.

Patient and public involvement Patients and/or the public were not involved in the design, or conduct, or reporting, or dissemination plans of this research.

Patient consent for publication Not applicable.

Ethics approval Not applicable.

Provenance and peer review Not commissioned; externally peer reviewed.

Data availability statement Data are available on reasonable request. All data relevant to the study are included in the article or uploaded as supplementary information.

ORCID iDs
Yang Yang http://orcid.org/0000-0002-0942-1800
Bin Gao http://orcid.org/0000-0002-0505-2972
Cynthia Ju http://orcid.org/0000-0002-1640-7169

REFERENCES

1 Dutkowski P, Linecker M, DeOliveira ML, *et al*. Challenges to liver transplantation and strategies to improve outcomes. *Gastroenterology* 2015;148:307–23.
2 Wertheim JA, Petrowsky H, Saab S, *et al*. Major challenges limiting liver transplantation in the United States. *Am J Transplant* 2011;11:1773–84.
3 Fellström B, Aküyrek LM, Backman U, *et al*. Postischemic reperfusion injury and allograft arteriosclerosis. *Transplant Proc* 1998;30:4278–80.
4 Howard TK, Klintmalm GB, Cofer JB, *et al*. The influence of preservation injury on rejection in the hepatic transplant recipient. *Transplantation* 1990;49:103–7.
5 Busuttil RW, Tanaka K. The utility of marginal donors in liver transplantation. *Liver Transpl* 2003;9:651–63.
6 Cameron AM, Ghobrial RM, Yersiz H, *et al*. Optimal utilization of donor grafts with extended criteria: a single-center experience in over 1000 liver transplants. *Ann Surg* 2006;243:discussion 53-5:748–53:.
7 Dar WA, Sullivan E, Bynon JS, *et al*. Ischaemia reperfusion injury in liver transplantation: cellular and molecular mechanisms. *Liver Int* 2019;39:788–801.
8 Durand F, Renz JF, Alkofer B, *et al*. Report of the Paris consensus meeting on expanded criteria donors in liver transplantation. *Liver Transpl* 2008;14:1694–707.
9 Park SW, Kim M, Brown KM, *et al*. Paneth cell-derived IL-17A causes multi-organ dysfunction after hepatic ischemia and reperfusion injury. *Hepatology* 2011;53:1662–75.
10 Bamboat ZM, Ocuin LM, Balachandran VP, *et al*. Conventional Dcs reduce liver ischemia/reperfusion injury in mice via IL-10 secretion. *J Clin Invest* 2010;120:40008:559–69:.
11 Nace GW, Huang H, Klune JR, *et al*. Cellular specific role of toll-like receptor 4 in hepatic ischemia-reperfusion injury. *Hepatology* 2013;58:374–87.
12 Galloway E, Shin T, Huber N, *et al*. Activation of hepatocytes by extracellular heat shock protein 72. *Am J Physiol Cell Physiol* 2008;295:C514–20.

13 Pittet JF, Morel DR, Mentha G, *et al*. Protective effect of indomethacin in the development of the Postreperfusion syndrome during liver transplantation in pigs. *Transplant Proc* 1991;23:2290–6.
14 Ke B, Shen X-D, Ji H, *et al*. HO-1-Stat3 axis in mouse liver ischemia/reperfusion injury: regulation of Tlr4 innate responses through Pi3K/PTEN signaling. *J Hepatol* 2012;56:359–66.
15 Ji H, Liu Y, Zhang Y, *et al*. T-cell immunoglobulin and Mucin domain 4 (TIM-4) signaling in innate immune-mediated liver ischemia-reperfusion injury. *Hepatology* 2014;60:2052–64.
16 Ke B, Shen X-D, Zhang Y, *et al*. Keap1-Nrf2 complex in ischemia-induced hepatocellular damage of mouse liver transplants. *J Hepatol* 2013;59:1200–7.
17 Kamo N, Ke B, Busuttil RW, *et al*. PTEN-mediated AKT/beta-Catenin/Foxo1 signaling regulates innate immune responses in mouse liver ischemia/reperfusion injury. *Hepatology* 2013;57:289–98.
18 Fabre V, Beiting DP, Bliss SK, *et al*. Eosinophil deficiency compromises parasite survival in chronic Nematode infection. *J Immunol* 2009;182:1577–83.
19 Klion AD, Nutman TB. The role of Eosinophils in host defense against Helminth parasites. *J Allergy Clin Immunol* 2004;113:30–7.
20 Gleich GJ. Mechanisms of eosinophil-associated inflammation. *J Allergy Clin Immunol* 2000;105:651–63.
21 Calhoun WJ, Sedgwick J, Busse WW. The role of Eosinophils in the pathophysiology of asthma. *Ann N Y Acad Sci* 1991;629:62–72.
22 Bousquet J, Chanez P, Lacoste JY, *et al*. Eosinophilic inflammation in asthma. *N Engl J Med* 1990;323:1033–9.
23 Lee JJ, Jacobsen EA, McGarry MP, *et al*. Eosinophils in health and disease: the LIAR hypothesis. *Clin Exp Allergy* 2010;40:563–75.
24 Tani Y, Isobe Y, Imoto Y, *et al*. Eosinophils control the resolution of inflammation and draining lymph node hypertrophy through the Proresolving mediators and Cxcl13 pathway in mice. *FASEB J* 2014;28:4036–43.
25 Yamada T, Tani Y, Nakanishi H, *et al*. Eosinophils promote resolution of acute Peritonitis by producing Proresolving mediators in mice. *FASEB J* 2011;25:561–8.
26 Heredia JE, Mukundan L, Chen FM, *et al*. Type 2 innate signals stimulate Fibro/Adipogenic progenitors to facilitate muscle regeneration. *Cell* 2013;153:376–88.
27 Vicetti Miguel RD, Quispe Calla NE, Dixon D, *et al*. IL-4-Secreting Eosinophils promote endometrial Stromal cell proliferation and prevent Chlamydia-induced upper genital tract damage. *Proc Natl Acad Sci U S A* 2017;114:E6892–901.
28 Xu J-Y, Jiang W-Y, Xiong Y-Y, *et al*. Interleukin-5-induced eosinophil population improves cardiac function after myocardial infarction. *Circulation* 2020;142.
29 Liu J, Yang C, Liu T, *et al*. Eosinophils improve cardiac function after myocardial infarction. *Nat Commun* 2020;11:6396.
30 Toor IS, Rückerl D, Mair I, *et al*. Eosinophil deficiency promotes aberrant repair and adverse remodeling following acute myocardial infarction. *JACC Basic Transl Sci* 2020;5:665–81.
31 Wang Y, Yang Y, Wang M, *et al*. Eosinophils attenuate hepatic ischemia-reperfusion injury in mice through St2-dependent IL-13 production. *Sci Transl Med* 2021;13:eabb6576.
32 Ochkur SI, Jacobsen EA, Protheroe CA, *et al*. Coexpression of IL-5 and Eotaxin-2 in mice creates an eosinophil-dependent model of respiratory inflammation with characteristics of severe asthma. *J Immunol* 2007;178:7879–89.
33 Ochkur SI, Protheroe CA, Li W, *et al*. Cys-Leukotrienes promote fibrosis in a mouse model of eosinophil-mediated respiratory inflammation. *Am J Respir Cell Mol Biol* 2013;49:1074–84.
34 Jacobsen EA, Lesuer WE, Willetts L, *et al*. Eosinophil activities modulate the immune/inflammatory character of allergic respiratory responses in mice. *Allergy* 2014;69:315–27.
35 Minutti CM, Jackson-Jones LH, García-Fojeda B, *et al*. Local amplifiers of IL-4Ralpha-mediated macrophage activation promote repair in lung and liver. *Science* 2017;356:1076–80.
36 Jackson-Jones LH, Rückerl D, Svedberg F, *et al*. IL-33 delivery induces Serous cavity macrophage proliferation independent of interleukin-4 receptor alpha. *Eur J Immunol* 2016;46:2311–21.
37 Jenkins SJ, Ruckerl D, Thomas GD, *et al*. IL-4 directly signals tissue-resident Macrophages to proliferate beyond Homeostatic levels controlled by CSF-1. *J Exp Med* 2013;210:2477–91.
38 Loke P, Gallagher I, Nair MG, *et al*. Alternative activation is an innate response to injury that requires Cd4+ T cells to be sustained during chronic infection. *J Immunol* 2007;179:3926–36.
39 Goh YPS, Henderson NC, Heredia JE, *et al*. Eosinophils Secrete IL-4 to facilitate liver regeneration. *Proc Natl Acad Sci U S A* 2013;110:9914–9.
40 Yin S, Wang H, Bertola A, *et al*. Activation of invariant natural killer T cells Impedes liver regeneration by way of both IFN-Gamma- and IL-4-dependent mechanisms. *Hepatology* 2014;60:1356–66.
41 Zhao D, Yang F, Wang Y, *et al*. Alk1 signaling is required for the homeostasis of Kupffer cells and prevention of bacterial infection. *J Clin Invest* 2022;132:e150489.
42 Sakai M, Troutman TD, Seidman JS, *et al*. Liver-derived signals Sequentially Reprogram myeloid enhancers to initiate and maintain Kupffer cell identity. *Immunity* 2019;51:655–70.
43 Scott CL, T'Jonck W, Martens L, *et al*. The transcription factor Zeb2 is required to maintain the tissue-specific identities of Macrophages. *Immunity* 2018;49:312–25.
44 Hossain M, Kubes P. Innate immune cells Orchestrate the repair of sterile injury in the liver and beyond. *Eur J Immunol* 2019;49:831–41.
45 Devitt A, Marshall LJ. The innate immune system and the clearance of apoptotic cells. *J Leukoc Biol* 2011;90:447–57.
46 Tanaka M, Nishitai G. Immune regulation by dead cell clearance. *Curr Top Microbiol Immunol* 2017;403:171–83.
47 Brazil JC, Quiros M, Nusrat A, *et al*. Innate immune cell-epithelial Crosstalk during wound repair. *J Clin Invest* 2019;129:2983–93.
48 Eming SA, Hammerschmidt M, Krieg T, *et al*. Interrelation of immunity and tissue repair or regeneration. *Semin Cell Dev Biol* 2009;20:517–27.
49 Guenin-Mace L, Konieczny P, Naik S. Immune-epithelial cross talk in regeneration and repair. *Annu Rev Immunol* 2023;41:207–28.
50 Harrell CR, Djonov V, Volarevic V. The cross-talk between Mesenchymal stem cells and immune cells in tissue repair and regeneration. *IJMS* 2021;22:2472.
51 Ribatti D, Crivellato E. Immune cells and angiogenesis. *J Cell Mol Med* 2009;13:2822–33.
52 Isobe Y, Kato T, Arita M. Emerging roles of Eosinophils and eosinophil-derived lipid mediators in the resolution of inflammation. *Front Immunol* 2012;3:270.
53 Xu L, Yang Y, Wen Y, *et al*. Hepatic recruitment of Eosinophils and their protective function during acute liver injury. *J Hepatol* 2022;77:344–52.
54 Bernink JH, Germar K, Spits H. The role of Ilc2 in pathology of type 2 inflammatory diseases. *Curr Opin Immunol* 2014;31:115–20.
55 Motomura Y, Morita H, Moro K, *et al*. Basophil-derived interleukin-4 controls the function of natural helper cells, a member of Ilc2S, in lung inflammation. *Immunity* 2014;40:758–71.
56 Martinez-Gonzalez I, Steer CA, Takei F. Lung Ilc2S link innate and adaptive responses in allergic inflammation. *Trends Immunol* 2015;36:189–95.
57 Feng D, Xiang X, Guan Y, *et al*. Monocyte-derived Macrophages Orchestrate multiple cell-type interactions to repair necrotic liver lesions in disease models. *J Clin Invest* 2023;133:e166954.
58 Wynn TA, Vannella KM. Macrophages in tissue repair, regeneration, and fibrosis. *Immunity* 2016;44:450–62.
59 Mosser DM, Hamidzadeh K, Goncalves R. Macrophages and the maintenance of homeostasis. *Cell Mol Immunol* 2021;18:579–87.
60 Ramirez-Pedraza M, Fernández M. Interplay between Macrophages and angiogenesis: A double-edged sword in liver disease. *Front Immunol* 2019;10:2882.
61 Chen F, Liu Z, Wu W, *et al*. An essential role for Th2-type responses in limiting acute tissue damage during experimental Helminth infection. *Nat Med* 2012;18:260–6.
62 Gordon S. Alternative activation of Macrophages. *Nat Rev Immunol* 2003;3:23–35.
63 Sadtler K, Estrellas K, Allen BW, *et al*. Developing a pro-Regenerative Biomaterial scaffold Microenvironment requires T helper 2 cells. *Science* 2016;352:366–70.
64 Chen J, Zeng F, Forrester SJ, *et al*. Expression and function of the Epidermal growth factor receptor in physiology and disease. *Physiol Rev* 2016;96:1025–69.
65 Dao DT, Anez-Bustillos L, Adam RM, *et al*. Heparin-binding Epidermal growth factor-like growth factor as a critical mediator of tissue repair and regeneration. *Am J Pathol* 2018;188:2446–56.
66 Kiso S, Kawata S, Tamura S, *et al*. Expression of heparin-binding EGF-like growth factor in rat liver injured by carbon tetrachloride or D-galactosamine. *Biochem Biophys Res Commun* 1996;220:285–8.
67 Takemura T, Yoshida Y, Kiso S, *et al*. Conditional knockout of heparin-binding Epidermal growth factor-like growth factor in the liver accelerates carbon tetrachloride-induced liver injury in mice. *Hepatol Res* 2013;43:384–93.
68 Khai NC, Takahashi T, Ushikoshi H, *et al*. In vivo hepatic HB-EGF gene Transduction inhibits Fas-induced liver injury and induces liver regeneration in mice: a comparative study to HGF. *J Hepatol* 2006;44:1046–54.
69 Sakamoto K, Khai NC, Wang Y, *et al*. Heparin-binding Epidermal growth factor-like growth factor and hepatocyte growth factor inhibit cholestatic liver injury in mice through different mechanisms. *Int J Mol Med* 2016;38:1673–82.
70 Besner G, Higashiyama S, Klagsbrun M. Isolation and characterization of a macrophage-derived heparin-binding growth factor. *Cell Regul* 1990;1:811–9.
71 Fu E, Liu T, Yu S, *et al*. M2 Macrophages reduce the Radiosensitivity of head and neck cancer by releasing HB-EGF. *Oncol Rep* 2020;44:698–710.
72 Carroll MJ, Kapur A, Felder M, *et al*. M2 Macrophages induce ovarian cancer cell proliferation via a heparin binding Epidermal growth factor/matrix metalloproteinase 9 Intercellular feedback loop. *Oncotarget* 2016;7:86608–20.
73 Wen H-J, Gao S, Wang Y, *et al*. Myeloid cell-derived HB-EGF drives tissue recovery after Pancreatitis. *Cell Mol Gastroenterol Hepatol* 2019;8:173–92.
74 Higashiyama S, Nanba D. ADAM-mediated Ectodomain shedding of HB-EGF in receptor cross-talk. *Biochim Biophys Acta* 2005;1751:110–7.
75 Takenobu H, Yamazaki A, Hirata M, *et al*. The Stress- and inflammatory cytokine-induced Ectodomain shedding of heparin-binding Epidermal growth factor-like growth factor is mediated by P38 MAPK, distinct from the 12-O-Tetradecanoylphorbol-13-Acetate- and Lysophosphatidic acid-induced signaling cascades. *J Biol Chem* 2003;278:17255–62.
76 Raab G, Klagsbrun M. Heparin-binding EGF-like growth factor. *Biochim Biophys Acta* 1997;1333:F179–99.

Supplementary Materials and Methods

Animals

C57Bl/6J (stock#000664), ΔdblGATA1(on C57Bl/6J background, stock#005653), Il-4$^{-/-}$(on C57Bl/6J background, stock#002253), Il-4/GFP-enhanced transcript (on BALB/c background, 4Get, stock#004190), Alb-Cre (on C57Bl/6J background, stock#035593), and Clec4f-Cre (on C57Bl/6J background, stock#033296), BALB/cJ (stock# 000651) and Il-4rα$^{-/-}$(on BALB/c background, stock#003514) mice were purchased from the Jackson Laboratory. Breeders of PHIL[1], iPHIL[2], Il-4/13$^{fl/fl}$eoCre mice (backcrossed to C57Bl/6J at least 10 generations) [3] were obtained from Dr. Elizabeth Jacobsen (Mayo Clinic Arizona). Il-4rα$^{flox/flox}$ mice [4] were generated by Dr. Frank Brombacher (University of Cape Town, South Africa) and provided by Dr. Brain Kim (Washington University School of Medicine). The Hb-egf$^{flox/flox}$ mice were generated by Dr. Eisuke Mekada (Osaka University, Japan) and provided by Dr. Raymond Harris (Vanderbilt University). Colonies of Il-4rα$^{fl/fl}$Alb-Cre$^{+/-}$, Il-4rα$^{fl/fl}$Clec4f-Cre$^{+/-}$, Hb-egf$^{fl/fl}$Clec4f-Cre$^{+/-}$ mice were generated and maintained in the University of Texas Health Science Center at Houston (UTHealth) animal facility. All experiments were performed according to the guidelines of the institutional animal care and use committee (IACUC) at UTHealth.

Hepatic ischemia-reperfusion (IR) surgery and animal experiments

Hepatic IR or sham surgeries were performed in 10- to 12-week-old male mice as previously reported[5]. Mice were anesthetized by intraperitoneal (i.p.) injection of sodium pentobarbital (60 mg/kg) and then positioned on their back on a heated surgery table to maintain body temperature. A midline laparotomy was made and an atraumatic clip was used to block blood flow to the left lateral and median lobes of the liver. After 60 minutes (mins) of partial hepatic ischemia, the clip was removed to start hepatic reperfusion. For the sham group, the same steps were followed without vascular blockage. Throughout the procedure, the surgical site for the mice was draped with warm saline-soaked gauze. Mice were sacrificed at various post-reperfusion time points to collect blood and ischemic lobes of the liver tissues for further analysis.

For eosinophil depletion, iPHIL mice and WT littermates were i.p. injected with diphtheria toxin (DT; 15 ng/g) 16h prior to (1st dose) and 6h after (2nd dose) hepatic IR surgery. For eosinophil adoptive transfer, 10x10^6 bone marrow-derived eosinophils (bmEos) were injected intravenously (i.v.) into recipient mice at 24h after liver ischemia surgery. Control mice were injected with saline. For IL-4 or IL-13 neutralization, mice were i.p. injected with anti-mouse IL-4 antibody (10

μg/mouse, clone: 11B11, BioLegend) or anti-mouse IL-13 antibody (10 μg/mouse, AF-413-NA, R&D Systems) on days 1 and 3 after liver ischemia surgery. Control mice were injected with IgG.

For exogenous IL-4 treatment, mice were i.p. injected with IL-4 complex (IL-4c), which consisted of recombinant IL-4 (5 μg, Peprotech) complexed with anti-IL-4 antibody (25μg, clone11b11, BioXcell)[6, 7, 8] or Phosphate Buffered Saline (PBS) control on days 1 and 3 after liver ischemia surgery. For exogenous IL-13 treatment, mice were i.p. injected with IL-13 complex (IL-13c), which consisted of recombinant IL-13 (5 μg, PeproTech) complexed with anti-IL-13 antibody (25 μg, clone: eBio13A, eBioscience)[8] or PBS control on days 1 and 3 after liver ischemia surgery. For recombinant mouse (rm) HB-EGF treatment, mice were i.p. injected with rmHB-EGF (Sigma-Aldrich) or PBS on days 1 and 3 after IR surgery.

Ex vivo culturing of mouse bone marrow-derived eosinophils (bmEos) and bone marrow-derived macrophages (BMDM)

The *ex vivo* culturing of mouse bmEos was performed as reported previously[9]. Bone marrow cells were collected from the femurs of mice and cultured at $5x10^6$/mL in RPMI 1640 (Corning Cellgro) containing 20% fetal bovine serum (Corning), penicillin/streptomycin (100x, Corning Cellgro), 2 mM glutamine (Invitrogen), 25 mM HEPES, 1x non-essential amino acids, 1 mM sodium pyruvate (Gibco), 50 μM β-mercaptoethanol (Sigma-Aldrich) and supplemented with 100 ng/mL stem-cell factor (SCF, PeproTech) and 100 ng/mL FLT3-Ligand (FLT3-L, PeproTech) from days 0 to 4. On days 4 and 9, the cells were washed and cultured in fresh medium containing 10 ng/mL recombinant mouse interleukin-5 (IL-5, PeproTech). On day 14, the cells were collected and used for adoptive transfer or cell culture experiments.

To generate BMDM, bone marrow cells were collected from the femurs of mice and cultured at a density of $3x10^6$/mL in Dulbecco's Modified Eagle Medium (DMEM) medium (Gibco) containing 20% fetal bovine serum (GenDEPOT), penicillin/streptomycin (100x, Corning Cellgro), 100 mM Sodium Pyruvate (Corning Cellgro), 50 μM β-mercaptoethanol (Sigma-Aldrich) and 10% L929-conditioned medium for 7 days. The cells were then collected for *in vitro* stimulation by recombinant IL-4 (20ng/ml, Peprotech) for 6h or 24h.

Assessments of liver injury and repair

Serum concentrations of alanine transaminase (ALT) and aspartate aminotransferase (AST) were detected using diagnostic assay kits from Teco Diagnostics following the manufacturer's protocols. Liver tissue sections from ischemic lobes were fixed in 10% formalin overnight, embedded in

paraffin, and cut into 5 μm sections. Liver sections were stained with hematoxylin and eosin (H&E) for the examination of necrotic areas. Further, the degree of liver injury was evaluated based on the Suzuki's criteria and graded according to a scale of 0-4[10]. 0, none congestion, none vacuolization and none necrosis; 1, minimal congestion, minimal vacuolization and single-cell necrosis; 2, mild congestion, mild vacuolization and <30% necrosis; 3, moderate congestion, moderate vacuolization and 30-40% necrosis; 4, severe congestion, severe vacuolization and >60% necrosis. IHC staining was performed using paraffin-embedded sections to determine Ki67 expression in the liver. Briefly, endogenous peroxidases were inactivated by 3% hydrogen peroxide. Nonspecific antigen binding was blocked using 2.5% horse serum. Rabbit monoclonal Ki67 antibody (#ab16667, Abcam) was used. After overnight incubation, the slides were incubated with a secondary antibody (HRP-Polymer, Vector laboratories) for 30 mins, followed by washing and staining with 3,3'-diaminobenzidine (DAB, Vector laboratories). The quantification of $Ki67^+$ proliferating hepatocytes and the detection of PCNA in liver tissues by immunoblotting were performed to determine the extents of liver regeneration and recovery after IR injury.

Isolation of liver non-parenchymal cells (NPCs)

Liver NPCs were isolated following a previously established method[9]. Liver tissues were perfused *in situ* with a perfusion buffer (1x *Hank's Balanced Salt Solution,* HBSS), followed by a digestion buffer (1x HBSS supplemented with 0.04% Collagenase type I, Sigma-Aldrich). Once digested, the liver was disrupted in an anti-coagulant-citrate-dextrose solution and the cells passed through a 70μm cell strainer. After filtering, cells were further purified using 35% Percoll (Sigma-Aldrich). The remaining red blood cells were neutralized in Ammonium-Chloride-Potassium (ACK) lysing buffer, which consists of NH_4Cl (150 mM), $KHCO_3$ (10 mM), and Na_2EDTA (0.1 mM) set to a pH range of 7.2-7.4.

Flow cytometry analysis

Cell surface staining was performed by incubating cells ($1x10^6$/per tube) with antibodies for 30 mins at 4°C after blocking with anti-CD16/CD32 (#101302, Biolegend). Dead cells were excluded by staining with blue fluorescent reactive dye (1:200, Invitrogen, #2176884). Flurochrome-conjugated antibodies against CD45 (1:200, clone 30-F11), CD11b (1:200, clone M1/70), Siglec-F (1:200, clone E50-2440), CCR3 (1:200, clone JO73E5), CD3 (1:200, clone 17A2), CD124 (1:200, IL-4Rα, clone mIL4R-M1), Clec4f (1:200, clone 3E3F9), IL-13 (1:100, clone eBio13A), CD45.1 (1:200, clone A20), CD31 (1:200, clone MEC13.3) and F4/80 (1:200, clone BM8) were purchased from eBioscience or BD Biosciences or Biolegend. For IL-13 intracellular staining,

NPCs were treated with 500 ng/mL ionomycin (Sigma-Aldrich) in the presence of GolgiPlug (BD) for 4h before staining with anti-IL-13 antibody using a Fixation & Permeabilization Kit (Invitrogen). The cells were analyzed using a CytoFLEX LX flow cytometer (Beckman Coulter) and the data was analyzed with FlowJo v10.7.

RNA isolation and quantitative real-time polymerase chain reaction (qRT-PCR)

Total RNA was purified from liver tissues or culture cells using Pure-Link RNA Mini Kit (Invitrogen) according to the manufacturer's protocol, and 1 μg RNA was reverse transcribed into cDNA using an iScript cDNA Synthesis Kit (Bio-Rad). Relative quantitative gene expression was measured with SYBR Green PCR Supermix from GenDEPOT. 18S rRNA was used as an internal standard. The primers used for qRT-PCR are listed in *Table S1*.

Western blotting

Liver tissues were homogenized in RIPA buffer (Thermo Fisher Scientific) containing protease and phosphatase inhibitor cocktail (Thermo Fisher Scientific). Protein concentrations were quantified with a BCA protein assay kit (Thermo Fisher Scientific). At least 30 μg of total protein from each sample were loaded and separated by gel electrophoresis and then transferred to nitrocellulose membranes. After blocking, membranes were incubated with primary antibodies at 4°C overnight. The primary antibodies recognizing PCNA (1:1000, #2586), phosphorylated-EGFR (1:1000, #3777), and total-EGFR (1:1000, #4267, Cell Signaling Technology) were purchased from Cell Signaling Technology. β-actin (1:8000, #A3854) was purchased from Sigma-Aldrich. The next day, the membranes were washed and incubated with HRP-conjugated secondary antibodies (anti-Rabbit, #7074, 1:5000, 1:5000, Cell Signaling Technology) or (anti-mouse, #7076, 1:5000, Cell Signaling Technology) at room temperature for 1 h. Proteins were visualized with the ECL chemiluminescent kit (ECL-plus, Thermo Scientific). Detection and quantification of protein bands were performed using a ChemiDoc Imaging System with ImageLab Software (BioRad Laboratories).

Enzyme-linked immunosorbent assay (ELISA)

BMDM from BALB/c wild-type mice or Il-4r$\alpha^{-/-}$mice were treated with or without IL-4 (20 ng/ml, Peprotech) for 24h at 37°C. The supernatants were then harvested to detect HB-EGF protein by ELISA (#DY8239-05, R&D systems) according to the manufacturer's protocols.

Statistical analysis

All statistical analyses and graphing were conducted with GraphPad Prism version 10.1.2 (GraphPad Software Inc.). Results were presented as mean ± SEM. For all comparisons in which there were two groups of values, a two-tailed unpaired Student's t-test with Welch's correction was performed after demonstrating that the data follow a normal distribution by the Shapiro-Wilk normality test. One-way ANOVA was used to compare values obtained from three or more groups with one independent variable, followed by Tukey's test. To compare groups with two independent variables, two-way ANOVA was used followed by Tukey's test. Differences in values were considered significant at $p<0.05$. All experiments were repeated a minimum of three times.

Reference:

1 Lee JJ, Dimina D, Macias MP, Ochkur SI, McGarry MP, O'Neill KR*, et al.* Defining a link with asthma in mice congenitally deficient in eosinophils. Science 2004;**305**:1773-6.
2 Jacobsen EA, Lesuer WE, Willetts L, Zellner KR, Mazzolini K, Antonios N*, et al.* Eosinophil activities modulate the immune/inflammatory character of allergic respiratory responses in mice. Allergy 2014;**69**:315-27.
3 Doyle AD, Mukherjee M, LeSuer WE, Bittner TB, Pasha SM, Frere JJ*, et al.* Eosinophil-derived IL-13 promotes emphysema. Eur Respir J 2019;**53**.
4 Herbert DR, Holscher C, Mohrs M, Arendse B, Schwegmann A, Radwanska M*, et al.* Alternative macrophage activation is essential for survival during schistosomiasis and downmodulates T helper 1 responses and immunopathology. Immunity 2004;**20**:623-35.
5 Abe Y, Hines IN, Zibari G, Pavlick K, Gray L, Kitagawa Y*, et al.* Mouse model of liver ischemia and reperfusion injury: method for studying reactive oxygen and nitrogen metabolites in vivo. Free Radic Biol Med 2009;**46**:1-7.
6 Minutti CM, Jackson-Jones LH, Garcia-Fojeda B, Knipper JA, Sutherland TE, Logan N*, et al.* Local amplifiers of IL-4Ralpha-mediated macrophage activation promote repair in lung and liver. Science 2017;**356**:1076-80.
7 Jackson-Jones LH, Ruckerl D, Svedberg F, Duncan S, Maizels RM, Sutherland TE*, et al.* IL-33 delivery induces serous cavity macrophage proliferation independent of interleukin-4 receptor alpha. Eur J Immunol 2016;**46**:2311-21.
8 Jenkins SJ, Ruckerl D, Thomas GD, Hewitson JP, Duncan S, Brombacher F*, et al.* IL-4 directly signals tissue-resident macrophages to proliferate beyond homeostatic levels controlled by CSF-1. J Exp Med 2013;**210**:2477-91.
9 Dyer KD, Moser JM, Czapiga M, Siegel SJ, Percopo CM, Rosenberg HF. Functionally competent eosinophils differentiated ex vivo in high purity from normal mouse bone marrow. J Immunol 2008;**181**:4004-9.
10 Suzuki S, Toledo-Pereyra LH, Rodriguez FJ, Cejalvo D. Neutrophil infiltration as an important factor in liver ischemia and reperfusion injury. Modulating effects of FK506 and cyclosporine. Transplantation 1993;**55**:1265-72.

Supplemental figures:

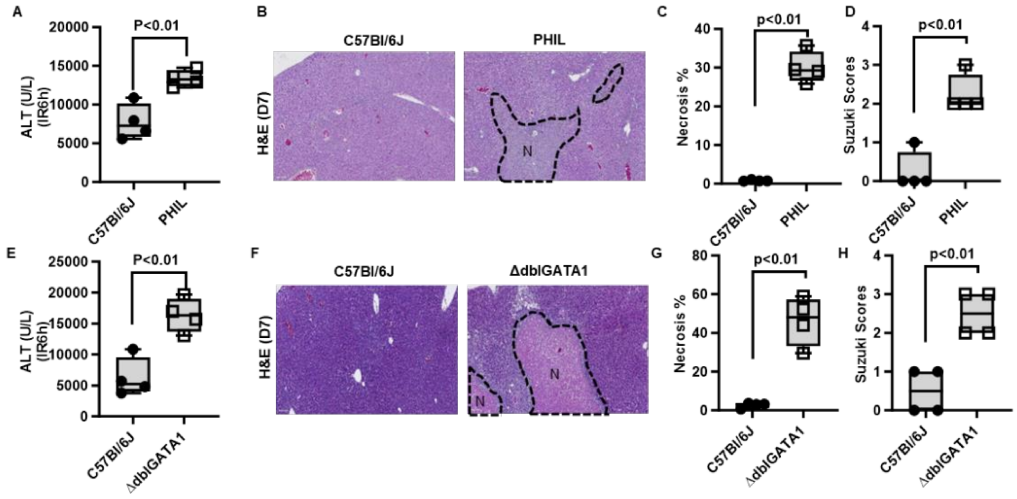

Fig. S1. Liver repair after IR injury is impaired in eosinophil-deficient mice. (A-D) Male PHIL mice and WT littermates were subjected to hepatic IR surgery (n=4/group). (E-H) Male ΔdblGATA-1 and WT C57Bl/6J mice were subjected to hepatic IR surgery (n=4/group). All mice were sacrificed on day 7 after IR surgery. (A, E) Serum ALT levels at 6h after IR surgery. (B, C and F, G) Liver necrosis (N, outlined areas) was evaluated and quantified on day 7 after IR surgery. (D, H) Liver pathology was assessed by using the Suzuki's scoring system on day 7 after IR surgery. Two-tailed unpaired Student's t-test with Welch's correction was performed in A, C, D, E, G, and H.

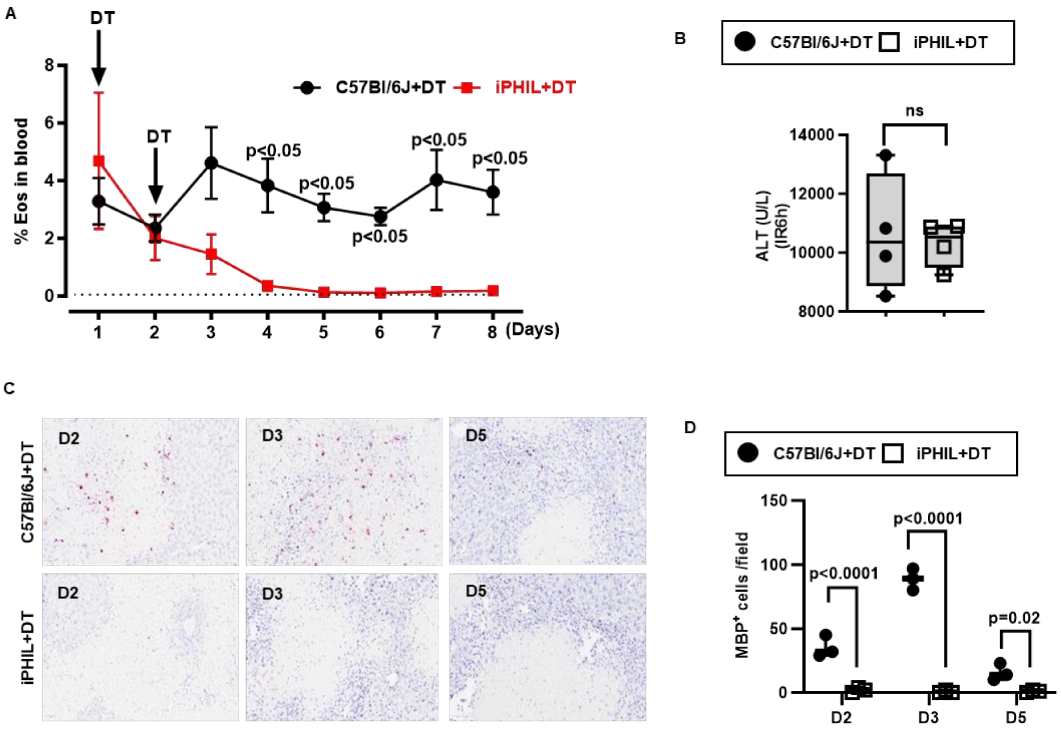

Fig. S2. Depletion of eosinophils in iPHIL mice. (A) Male iPHIL mice and WT littermates (C57Bl/6J) were injected i.p. with DT (5ng/g mouse) on day 1 and day 2. Blood eosinophils were analyzed by flow cytometry from day 1 to day 8 (n=3/group). (B) Male iPHIL mice and WT littermates were subjected to hepatic IR surgery. Mice were administered (i.p.) the first dose of DT at 16h prior to IR surgery and the second dose at 6h after surgery. Serum ALT levels were measured at 6h after IR surgery (n=4/group). (C-D) iPHIL mice and WT littermates were i.p. injected with DT at 16h prior to and 6h after hepatic IR surgery. Mice were sacrificed on days 2, 3, and 5 after IR surgery. IHC staining for eosinophils by anti-MBP antibody and the numbers of MBP^+ cells quantified (n=3/group). Two-tailed unpaired Student's t-test with Welch's correction was performed in A, B and D.

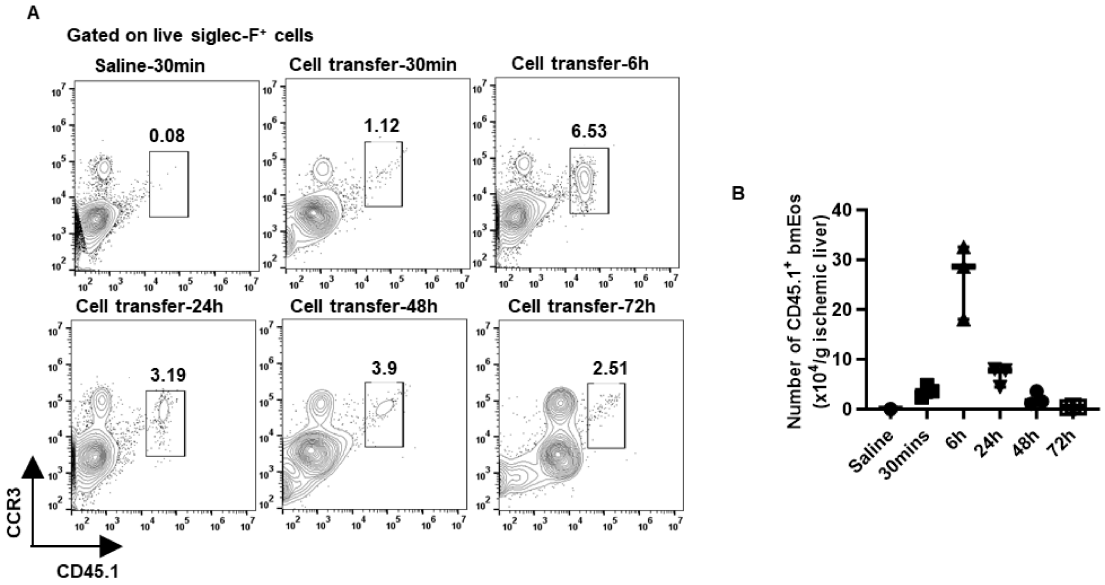

Fig. S3. Detection of bmEos in the liver after adoptive transfer. C57Bl/6J (CD45.2) mice were subjected to hepatic IR surgery and after 1 day injected with bmEos ($10x10^6$) obtained from B6-CD45.1 mice. Control mice were injected with saline. The numbers of transferred bmEos ($CD45.1^+$ $SiglecF^+CCR3^+$) in the liver of recipient mice were measured by flow cytometry at 6h, 24h, 48h, and 72h after adoptive transfer of the cells (n=3/group).

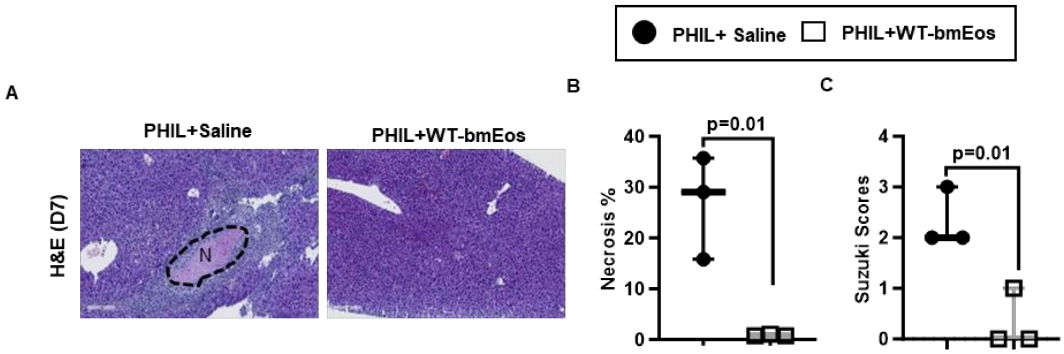

Fig. S4. Adoptive transfer of WT eosinophils to PHIL mice restores liver repair after IR injury. Male PHIL mice were subjected to hepatic IR surgery and after 1 day injected with WT-bmEos ($10x10^6$). Control mice were injected with saline. All mice were sacrificed on day 7 after IR surgery (n=3/group). (A, B) Liver necrosis (N, outlined areas) was evaluated and quantified. (C) Liver pathology was assessed by using the Suzuki's scoring system. Two-tailed unpaired Student's t-test with Welch's correction was performed in B and C.

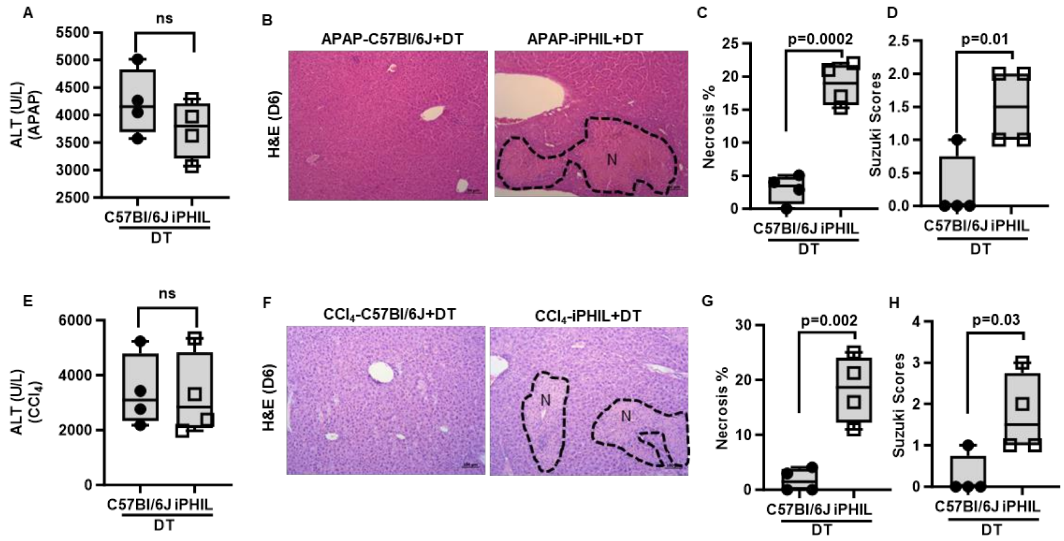

Fig. S5. Liver repair is delayed in iPHIL mice after APAP and CCl_4 treatment. (A-H) Male iPHIL mice and their WT littermates were i.p. injected with APAP or CCl_4. For APAP treatment, mice were fasted overnight before injected intraperitoneally i.p. with APAP. Mice were treated with 210 mg/kg of APAP. For CCl_4 treatment, a 1:4 dilution of 1 ml/kg CCl_4 in corn oil was i.p. injected to mice. All mice were administered (i.p.) the first dose of DT at 16h prior to APAP or CCl_4 treatment. They were then injected with a second dose of DT at 8h after APAP injection or 12h after CCl_4 injection. All mice were sacrificed on day 6 (n=4/group). (A, E) Serum ALT levels at 8h after APAP treatment and 12h after CCl_4 treatment. (B, C and F, G) Liver necrosis (N, outlined areas) was evaluated and quantified. (D, H) Liver pathology was assessed by using the Suzuki's scoring system. Two-tailed unpaired Student's t-test with Welch's correction was performed in A, C, D, E, G, and H.

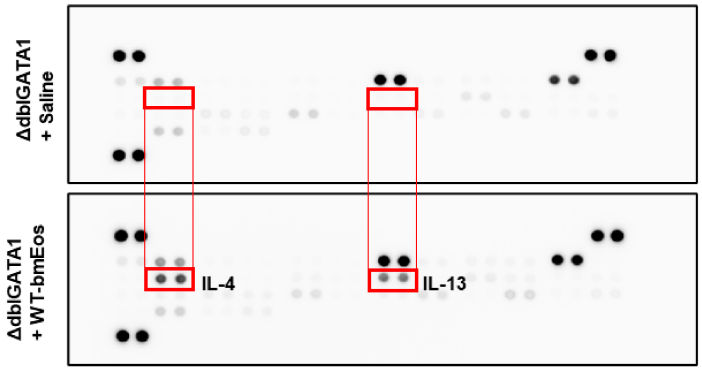

Fig. S6. Adoptive transfer of WT bmEos to ΔdblGATA-1 mice increased hepatic levels of IL-4 and IL-13. 6 Male ΔdblGATA-1 were subjected to hepatic IR surgery. After 24h, half of the mice were i.v. injected with bmEos ($10x10^6$) and the other half injected with saline as control. Mice were sacrificed after 3 days, and the expression levels of 40 cytokines in the liver samples were measured by using a Proteome Profiler Mouse Cytokine Array Kit. Data are representative of three independent experiments.

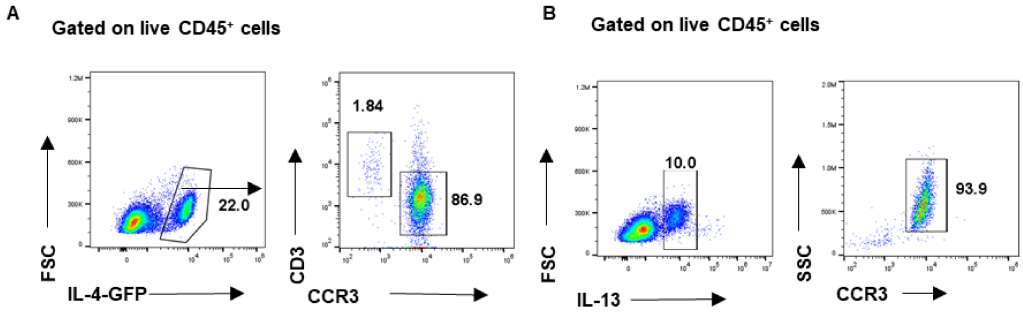

Fig. S7. IL-4 and IL-13 production by hepatic eosinophils during liver IR injury. (A, B) Male 4Get mice were subjected to hepatic IR injury and sacrificed after 3 days. Liver NPCs were isolated and stained intracellularly for IL-13. The IL-4-GFP$^+$ cells and IL-13$^+$ cells were gated. The proportions of IL-4$^+$ or IL-13$^+$ cells that were eosinophils (CCR3$^+$) are shown. Data are representative of three independent experiments.

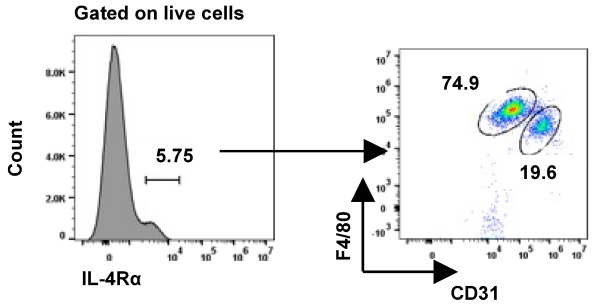

Fig. S8. Liver macrophages express IL-4Rα. Liver NPCs were isolated from naïve C57Bl/6J mice and analyzed by flow cytometry. IL-4Rα$^+$ cells were gated and identified as macrophages (F4/80$^+$, 74.9%) and LSECs (CD31$^+$, 19.6%). Data are representative of three independent experiments.

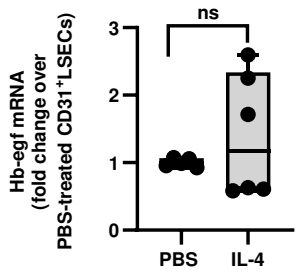

Fig.S9. IL-4 does not induce Hb-egf mRNA expression in liver sinusoidal endothelial cells (LSECs). LSECs were purified from naïve C57Bl/6J mice by magnetic-associated cell sorting (MACS) using anti-CD31 antibody. The cells were stimulated with IL-4 (10ng/ml) or PBS as the control for 6h (n=5-6/group). The mRNA levels of Hb-egf were measured by q-PCR. A two-tailed unpaired Student's t-test with Welch's correction was performed.

Table S1: Primer sequences for qRT-PCR

Gene Name (Symbol)	Forward Sequence	Reverse Sequence
Mouse Hb-egf	CGGGGAGTGCAGATACCTG	TTCTCCACTGGTAGAGTCAGC
Mouse Areg	GGTCTTAGGCTCAGGCCATTA	CGCTTATGGTGGAAACCTCTC
Mouse Tgf-α	CACTCTGGGTACGTGGGTG	CACAGGTGATAATGAGGACAGC
Mouse Btc	AATTCTCCACTGTGTGGTAGCA	GGTTTTCACTTTCTGTCTAGGGG
Mouse Ereg	CTGCCTCTTGGGTCTTGACG	GCGGTACAGTTATCCTCGGATTC
Mouse Epgn	GGGGGTTCTGATAGCAGTCTG	TCGGTGTTGTTAAATGTCCAGTT
Mouse Egf	AGAGCATCTCTCGGATTGACC	CCCGTTAAGGAAAACTCTTAGCA
Mouse 18s	ACGGAAGGGCACCACCAGGA	CACCACCACCCACGGAATCG

Supplementary Materials and Methods

Animals

C57Bl/6J (stock#000664), ΔdblGATA1(on C57Bl/6J background, stock#005653), Il-4$^{-/-}$(on C57Bl/6J background, stock#002253), Il-4/GFP-enhanced transcript (on BALB/c background, 4Get, stock#004190), Alb-Cre (on C57Bl/6J background, stock#035593), and Clec4f-Cre (on C57Bl/6J background, stock#033296), BALB/cJ (stock# 000651) and Il-4rα$^{-/-}$(on BALB/c background, stock#003514) mice were purchased from the Jackson Laboratory. Breeders of PHIL[1], iPHIL[2], Il-4/13$^{fl/fl}$eoCre mice (backcrossed to C57Bl/6J at least 10 generations) [3] were obtained from Dr. Elizabeth Jacobsen (Mayo Clinic Arizona). Il-4rα$^{flox/flox}$ mice [4] were generated by Dr. Frank Brombacher (University of Cape Town, South Africa) and provided by Dr. Brain Kim (Washington University School of Medicine). The Hb-egf$^{flox/flox}$ mice were generated by Dr. Eisuke Mekada (Osaka University, Japan) and provided by Dr. Raymond Harris (Vanderbilt University). Colonies of Il-4rα$^{fl/fl}$Alb-Cre$^{+/-}$, Il-4rα$^{fl/fl}$Clec4f-Cre$^{+/-}$, Hb-egf$^{fl/fl}$Clec4f-Cre$^{+/-}$ mice were generated and maintained in the University of Texas Health Science Center at Houston (UTHealth) animal facility. All experiments were performed according to the guidelines of the institutional animal care and use committee (IACUC) at UTHealth.

Hepatic ischemia-reperfusion (IR) surgery and animal experiments

Hepatic IR or sham surgeries were performed in 10- to 12-week-old male mice as previously reported[5]. Mice were anesthetized by intraperitoneal (i.p.) injection of sodium pentobarbital (60 mg/kg) and then positioned on their back on a heated surgery table to maintain body temperature. A midline laparotomy was made and an atraumatic clip was used to block blood flow to the left lateral and median lobes of the liver. After 60 minutes (mins) of partial hepatic ischemia, the clip was removed to start hepatic reperfusion. For the sham group, the same steps were followed without vascular blockage. Throughout the procedure, the surgical site for the mice was draped with warm saline-soaked gauze. Mice were sacrificed at various post-reperfusion time points to collect blood and ischemic lobes of the liver tissues for further analysis.

For eosinophil depletion, iPHIL mice and WT littermates were i.p. injected with diphtheria toxin (DT; 15 ng/g) 16h prior to (1st dose) and 6h after (2nd dose) hepatic IR surgery. For eosinophil adoptive transfer, 10x10^6 bone marrow-derived eosinophils (bmEos) were injected intravenously (i.v.) into recipient mice at 24h after liver ischemia surgery. Control mice were injected with saline. For IL-4 or IL-13 neutralization, mice were i.p. injected with anti-mouse IL-4 antibody (10

μg/mouse, clone: 11B11, BioLegend) or anti-mouse IL-13 antibody (10 μg/mouse, AF-413-NA, R&D Systems) on days 1 and 3 after liver ischemia surgery. Control mice were injected with IgG.

For exogenous IL-4 treatment, mice were i.p. injected with IL-4 complex (IL-4c), which consisted of recombinant IL-4 (5 μg, Peprotech) complexed with anti-IL-4 antibody (25μg, clone11b11, BioXcell)[6, 7, 8] or Phosphate Buffered Saline (PBS) control on days 1 and 3 after liver ischemia surgery. For exogenous IL-13 treatment, mice were i.p. injected with IL-13 complex (IL-13c), which consisted of recombinant IL-13 (5 μg, PeproTech) complexed with anti-IL-13 antibody (25 μg, clone: eBio13A, eBioscience)[8] or PBS control on days 1 and 3 after liver ischemia surgery. For recombinant mouse (rm) HB-EGF treatment, mice were i.p. injected with rmHB-EGF (Sigma-Aldrich) or PBS on days 1 and 3 after IR surgery.

Ex vivo culturing of mouse bone marrow-derived eosinophils (bmEos) and bone marrow-derived macrophages (BMDM)

The *ex vivo* culturing of mouse bmEos was performed as reported previously[9]. Bone marrow cells were collected from the femurs of mice and cultured at $5x10^6$/mL in RPMI 1640 (Corning Cellgro) containing 20% fetal bovine serum (Corning), penicillin/streptomycin (100x, Corning Cellgro), 2 mM glutamine (Invitrogen), 25 mM HEPES, 1x non-essential amino acids, 1 mM sodium pyruvate (Gibco), 50 μM β-mercaptoethanol (Sigma-Aldrich) and supplemented with 100 ng/mL stem-cell factor (SCF, PeproTech) and 100 ng/mL FLT3-Ligand (FLT3-L, PeproTech) from days 0 to 4. On days 4 and 9, the cells were washed and cultured in fresh medium containing 10 ng/mL recombinant mouse interleukin-5 (IL-5, PeproTech). On day 14, the cells were collected and used for adoptive transfer or cell culture experiments.

To generate BMDM, bone marrow cells were collected from the femurs of mice and cultured at a density of $3x10^6$/mL in Dulbecco's Modified Eagle Medium (DMEM) medium (Gibco) containing 20% fetal bovine serum (GenDEPOT), penicillin/streptomycin (100x, Corning Cellgro), 100 mM Sodium Pyruvate (Corning Cellgro), 50 μM β-mercaptoethanol (Sigma-Aldrich) and 10% L929-conditioned medium for 7 days. The cells were then collected for *in vitro* stimulation by recombinant IL-4 (20ng/ml, Peprotech) for 6h or 24h.

Assessments of liver injury and repair

Serum concentrations of alanine transaminase (ALT) and aspartate aminotransferase (AST) were detected using diagnostic assay kits from Teco Diagnostics following the manufacturer's protocols. Liver tissue sections from ischemic lobes were fixed in 10% formalin overnight, embedded in

paraffin, and cut into 5 μm sections. Liver sections were stained with hematoxylin and eosin (H&E) for the examination of necrotic areas. Further, the degree of liver injury was evaluated based on the Suzuki's criteria and graded according to a scale of 0-4[10]. 0, none congestion, none vacuolization and none necrosis; 1, minimal congestion, minimal vacuolization and single-cell necrosis; 2, mild congestion, mild vacuolization and <30% necrosis; 3, moderate congestion, moderate vacuolization and 30-40% necrosis; 4, severe congestion, severe vacuolization and >60% necrosis. IHC staining was performed using paraffin-embedded sections to determine Ki67 expression in the liver. Briefly, endogenous peroxidases were inactivated by 3% hydrogen peroxide. Nonspecific antigen binding was blocked using 2.5% horse serum. Rabbit monoclonal Ki67 antibody (#ab16667, Abcam) was used. After overnight incubation, the slides were incubated with a secondary antibody (HRP-Polymer, Vector laboratories) for 30 mins, followed by washing and staining with 3,3'-diaminobenzidine (DAB, Vector laboratories). The quantification of $Ki67^+$ proliferating hepatocytes and the detection of PCNA in liver tissues by immunoblotting were performed to determine the extents of liver regeneration and recovery after IR injury.

Isolation of liver non-parenchymal cells (NPCs)

Liver NPCs were isolated following a previously established method[9]. Liver tissues were perfused *in situ* with a perfusion buffer (1x *Hank's Balanced Salt Solution,* HBSS), followed by a digestion buffer (1x HBSS supplemented with 0.04% Collagenase type I, Sigma-Aldrich). Once digested, the liver was disrupted in an anti-coagulant-citrate-dextrose solution and the cells passed through a 70μm cell strainer. After filtering, cells were further purified using 35% Percoll (Sigma-Aldrich). The remaining red blood cells were neutralized in Ammonium-Chloride-Potassium (ACK) lysing buffer, which consists of NH_4Cl (150 mM), $KHCO_3$ (10 mM), and Na_2EDTA (0.1 mM) set to a pH range of 7.2-7.4.

Flow cytometry analysis

Cell surface staining was performed by incubating cells ($1x10^6$/per tube) with antibodies for 30 mins at 4°C after blocking with anti-CD16/CD32 (#101302, Biolegend). Dead cells were excluded by staining with blue fluorescent reactive dye (1:200, Invitrogen, #2176884). Flurochrome-conjugated antibodies against CD45 (1:200, clone 30-F11), CD11b (1:200, clone M1/70), Siglec-F (1:200, clone E50-2440), CCR3 (1:200, clone JO73E5), CD3 (1:200, clone 17A2), CD124 (1:200, IL-4Rα, clone mIL4R-M1), Clec4f (1:200, clone 3E3F9), IL-13 (1:100, clone eBio13A), CD45.1 (1:200, clone A20), CD31 (1:200, clone MEC13.3) and F4/80 (1:200, clone BM8) were purchased from eBioscience or BD Biosciences or Biolegend. For IL-13 intracellular staining,

NPCs were treated with 500 ng/mL ionomycin (Sigma-Aldrich) in the presence of GolgiPlug (BD) for 4h before staining with anti-IL-13 antibody using a Fixation & Permeabilization Kit (Invitrogen). The cells were analyzed using a CytoFLEX LX flow cytometer (Beckman Coulter) and the data was analyzed with FlowJo v10.7.

RNA isolation and quantitative real-time polymerase chain reaction (qRT-PCR)

Total RNA was purified from liver tissues or culture cells using Pure-Link RNA Mini Kit (Invitrogen) according to the manufacturer's protocol, and 1 μg RNA was reverse transcribed into cDNA using an iScript cDNA Synthesis Kit (Bio-Rad). Relative quantitative gene expression was measured with SYBR Green PCR Supermix from GenDEPOT. 18S rRNA was used as an internal standard. The primers used for qRT-PCR are listed in *Table S1*.

Western blotting

Liver tissues were homogenized in RIPA buffer (Thermo Fisher Scientific) containing protease and phosphatase inhibitor cocktail (Thermo Fisher Scientific). Protein concentrations were quantified with a BCA protein assay kit (Thermo Fisher Scientific). At least 30 μg of total protein from each sample were loaded and separated by gel electrophoresis and then transferred to nitrocellulose membranes. After blocking, membranes were incubated with primary antibodies at 4°C overnight. The primary antibodies recognizing PCNA (1:1000, #2586), phosphorylated-EGFR (1:1000, #3777), and total-EGFR (1:1000, #4267, Cell Signaling Technology) were purchased from Cell Signaling Technology. β-actin (1:8000, #A3854) was purchased from Sigma-Aldrich. The next day, the membranes were washed and incubated with HRP-conjugated secondary antibodies (anti-Rabbit, #7074, 1:5000, 1:5000, Cell Signaling Technology) or (anti-mouse, #7076, 1:5000, Cell Signaling Technology) at room temperature for 1 h. Proteins were visualized with the ECL chemiluminescent kit (ECL-plus, Thermo Scientific). Detection and quantification of protein bands were performed using a ChemiDoc Imaging System with ImageLab Software (BioRad Laboratories).

Enzyme-linked immunosorbent assay (ELISA)

BMDM from BALB/c wild-type mice or Il-4r$\alpha^{-/-}$mice were treated with or without IL-4 (20 ng/ml, Peprotech) for 24h at 37°C. The supernatants were then harvested to detect HB-EGF protein by ELISA (#DY8239-05, R&D systems) according to the manufacturer's protocols.

Statistical analysis

All statistical analyses and graphing were conducted with GraphPad Prism version 10.1.2 (GraphPad Software Inc.). Results were presented as mean ± SEM. For all comparisons in which there were two groups of values, a two-tailed unpaired Student's t-test with Welch's correction was performed after demonstrating that the data follow a normal distribution by the Shapiro-Wilk normality test. One-way ANOVA was used to compare values obtained from three or more groups with one independent variable, followed by Tukey's test. To compare groups with two independent variables, two-way ANOVA was used followed by Tukey's test. Differences in values were considered significant at $p<0.05$. All experiments were repeated a minimum of three times.

Reference:

1 Lee JJ, Dimina D, Macias MP, Ochkur SI, McGarry MP, O'Neill KR*, et al.* Defining a link with asthma in mice congenitally deficient in eosinophils. Science 2004;**305**:1773-6.
2 Jacobsen EA, Lesuer WE, Willetts L, Zellner KR, Mazzolini K, Antonios N*, et al.* Eosinophil activities modulate the immune/inflammatory character of allergic respiratory responses in mice. Allergy 2014;**69**:315-27.
3 Doyle AD, Mukherjee M, LeSuer WE, Bittner TB, Pasha SM, Frere JJ*, et al.* Eosinophil-derived IL-13 promotes emphysema. Eur Respir J 2019;**53**.
4 Herbert DR, Holscher C, Mohrs M, Arendse B, Schwegmann A, Radwanska M*, et al.* Alternative macrophage activation is essential for survival during schistosomiasis and downmodulates T helper 1 responses and immunopathology. Immunity 2004;**20**:623-35.
5 Abe Y, Hines IN, Zibari G, Pavlick K, Gray L, Kitagawa Y*, et al.* Mouse model of liver ischemia and reperfusion injury: method for studying reactive oxygen and nitrogen metabolites in vivo. Free Radic Biol Med 2009;**46**:1-7.
6 Minutti CM, Jackson-Jones LH, Garcia-Fojeda B, Knipper JA, Sutherland TE, Logan N*, et al.* Local amplifiers of IL-4Ralpha-mediated macrophage activation promote repair in lung and liver. Science 2017;**356**:1076-80.
7 Jackson-Jones LH, Ruckerl D, Svedberg F, Duncan S, Maizels RM, Sutherland TE*, et al.* IL-33 delivery induces serous cavity macrophage proliferation independent of interleukin-4 receptor alpha. Eur J Immunol 2016;**46**:2311-21.
8 Jenkins SJ, Ruckerl D, Thomas GD, Hewitson JP, Duncan S, Brombacher F*, et al.* IL-4 directly signals tissue-resident macrophages to proliferate beyond homeostatic levels controlled by CSF-1. J Exp Med 2013;**210**:2477-91.
9 Dyer KD, Moser JM, Czapiga M, Siegel SJ, Percopo CM, Rosenberg HF. Functionally competent eosinophils differentiated ex vivo in high purity from normal mouse bone marrow. J Immunol 2008;**181**:4004-9.
10 Suzuki S, Toledo-Pereyra LH, Rodriguez FJ, Cejalvo D. Neutrophil infiltration as an important factor in liver ischemia and reperfusion injury. Modulating effects of FK506 and cyclosporine. Transplantation 1993;**55**:1265-72.

Supplemental figures:

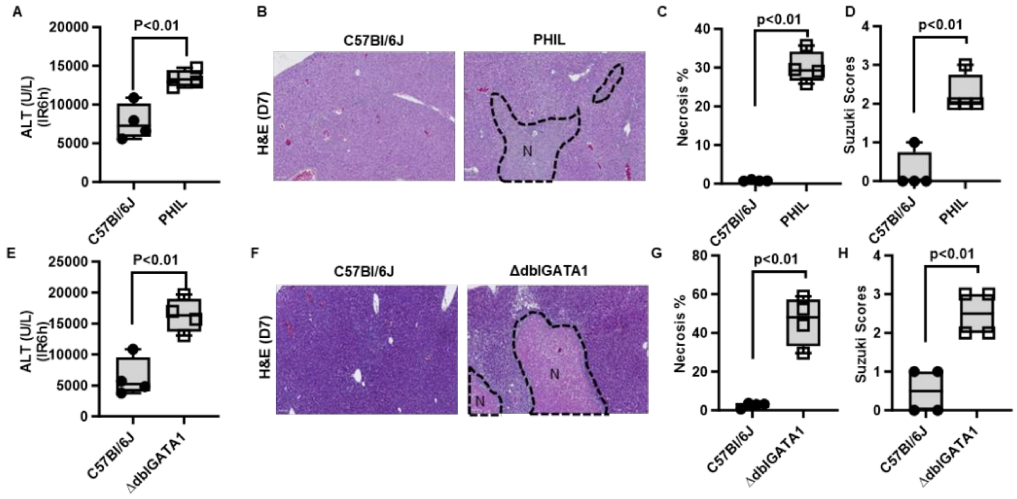

Fig. S1. Liver repair after IR injury is impaired in eosinophil-deficient mice. (A-D) Male PHIL mice and WT littermates were subjected to hepatic IR surgery (n=4/group). (E-H) Male ΔdblGATA-1 and WT C57Bl/6J mice were subjected to hepatic IR surgery (n=4/group). All mice were sacrificed on day 7 after IR surgery. (A, E) Serum ALT levels at 6h after IR surgery. (B, C and F, G) Liver necrosis (N, outlined areas) was evaluated and quantified on day 7 after IR surgery. (D, H) Liver pathology was assessed by using the Suzuki's scoring system on day 7 after IR surgery. Two-tailed unpaired Student's t-test with Welch's correction was performed in A, C, D, E, G, and H.

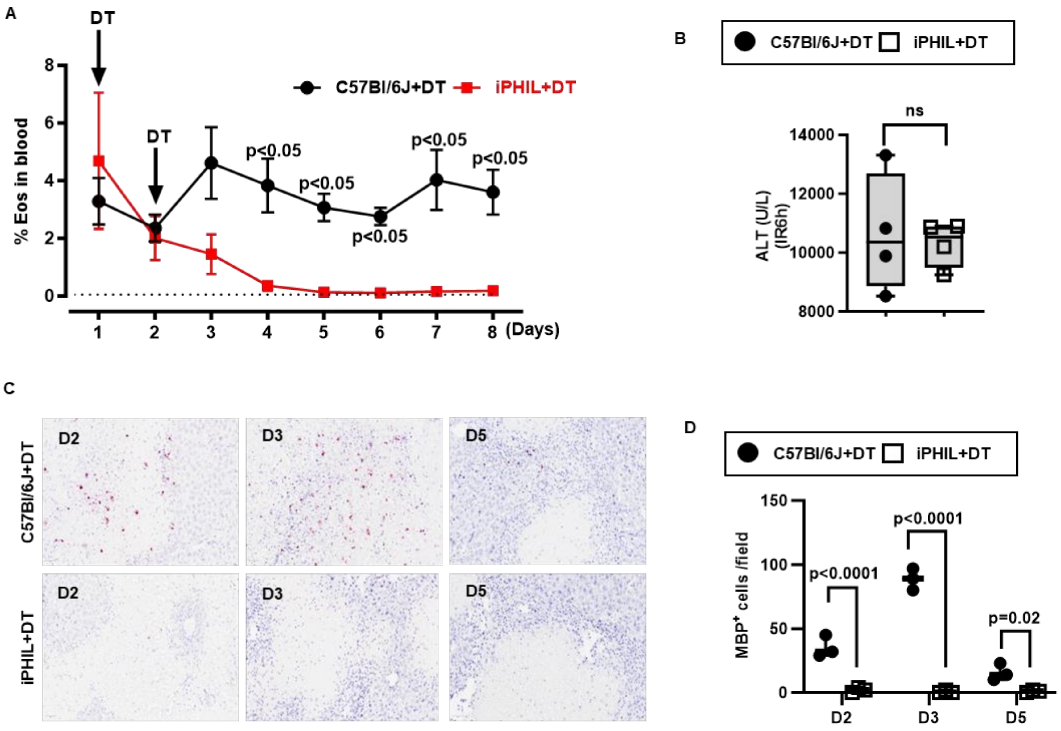

Fig. S2. Depletion of eosinophils in iPHIL mice. (A) Male iPHIL mice and WT littermates (C57Bl/6J) were injected i.p. with DT (5ng/g mouse) on day 1 and day 2. Blood eosinophils were analyzed by flow cytometry from day 1 to day 8 (n=3/group). (B) Male iPHIL mice and WT littermates were subjected to hepatic IR surgery. Mice were administered (i.p.) the first dose of DT at 16h prior to IR surgery and the second dose at 6h after surgery. Serum ALT levels were measured at 6h after IR surgery (n=4/group). (C-D) iPHIL mice and WT littermates were i.p. injected with DT at 16h prior to and 6h after hepatic IR surgery. Mice were sacrificed on days 2, 3, and 5 after IR surgery. IHC staining for eosinophils by anti-MBP antibody and the numbers of MBP^+ cells quantified (n=3/group). Two-tailed unpaired Student's t-test with Welch's correction was performed in A, B and D.

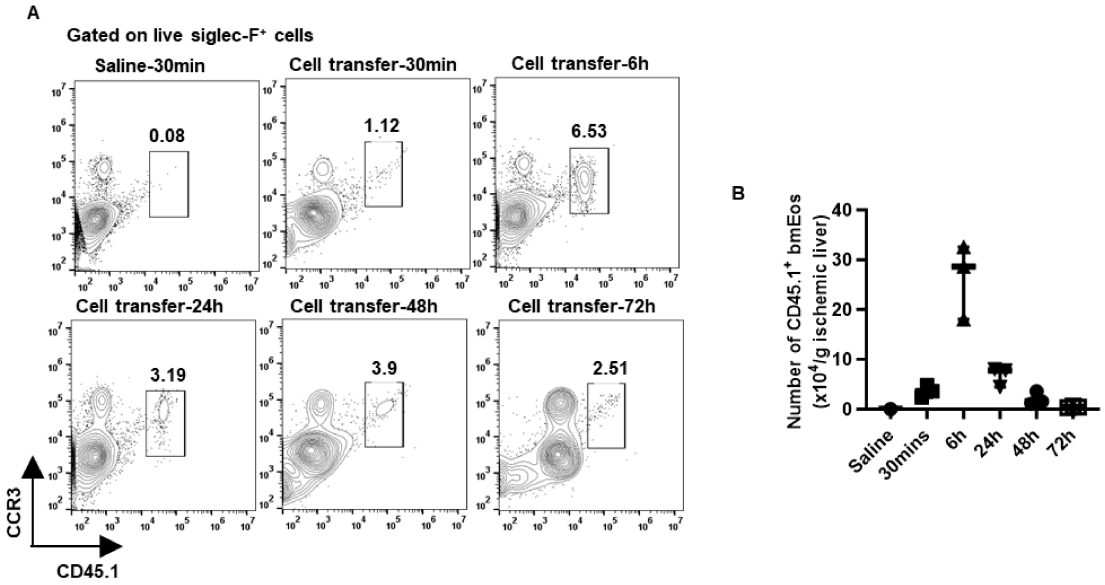

Fig. S3. Detection of bmEos in the liver after adoptive transfer. C57Bl/6J (CD45.2) mice were subjected to hepatic IR surgery and after 1 day injected with bmEos ($10x10^6$) obtained from B6-CD45.1 mice. Control mice were injected with saline. The numbers of transferred bmEos ($CD45.1^+$ $SiglecF^+CCR3^+$) in the liver of recipient mice were measured by flow cytometry at 6h, 24h, 48h, and 72h after adoptive transfer of the cells (n=3/group).

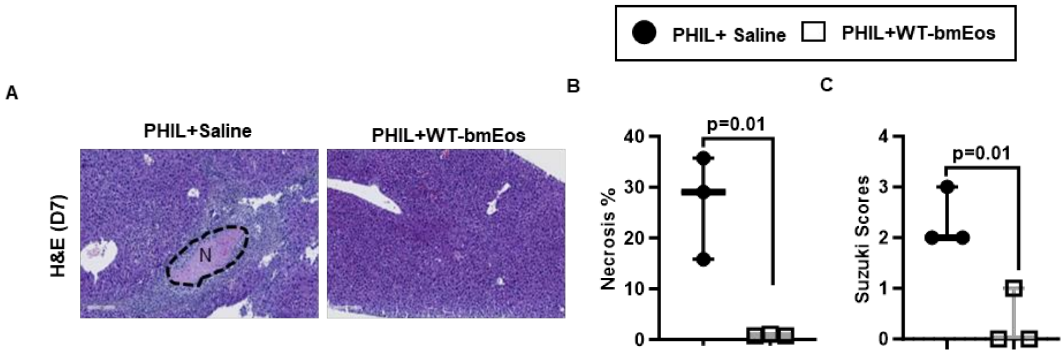

Fig. S4. Adoptive transfer of WT eosinophils to PHIL mice restores liver repair after IR injury. Male PHIL mice were subjected to hepatic IR surgery and after 1 day injected with WT-bmEos ($10x10^6$). Control mice were injected with saline. All mice were sacrificed on day 7 after IR surgery (n=3/group). (A, B) Liver necrosis (N, outlined areas) was evaluated and quantified. (C) Liver pathology was assessed by using the Suzuki's scoring system. Two-tailed unpaired Student's t-test with Welch's correction was performed in B and C.

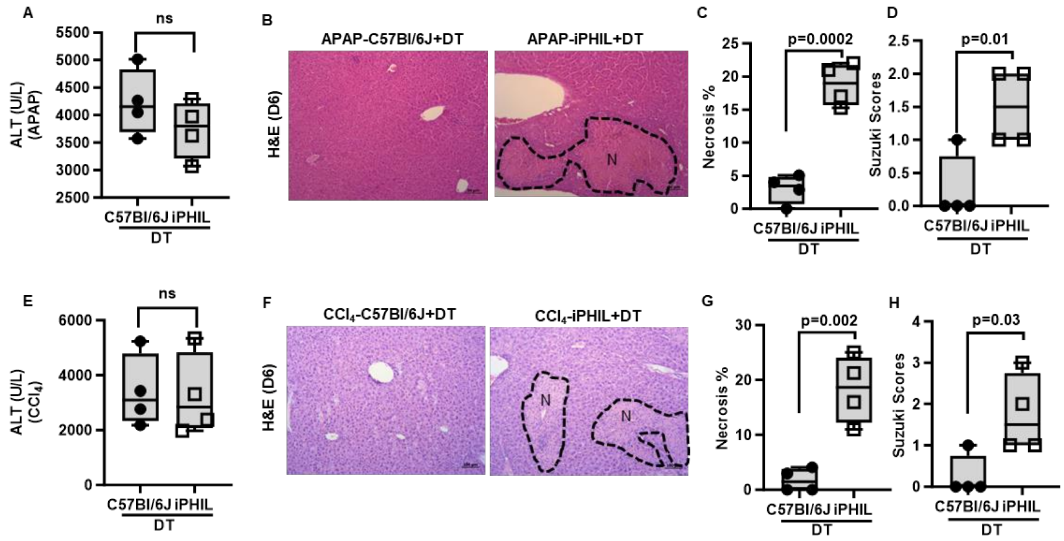

Fig. S5. Liver repair is delayed in iPHIL mice after APAP and CCl_4 treatment. (A-H) Male iPHIL mice and their WT littermates were i.p. injected with APAP or CCl_4. For APAP treatment, mice were fasted overnight before injected intraperitoneally i.p. with APAP. Mice were treated with 210 mg/kg of APAP. For CCl_4 treatment, a 1:4 dilution of 1 ml/kg CCl_4 in corn oil was i.p. injected to mice. All mice were administered (i.p.) the first dose of DT at 16h prior to APAP or CCl_4 treatment. They were then injected with a second dose of DT at 8h after APAP injection or 12h after CCl_4 injection. All mice were sacrificed on day 6 (n=4/group). (A, E) Serum ALT levels at 8h after APAP treatment and 12h after CCl_4 treatment. (B, C and F, G) Liver necrosis (N, outlined areas) was evaluated and quantified. (D, H) Liver pathology was assessed by using the Suzuki's scoring system. Two-tailed unpaired Student's t-test with Welch's correction was performed in A, C, D, E, G, and H.

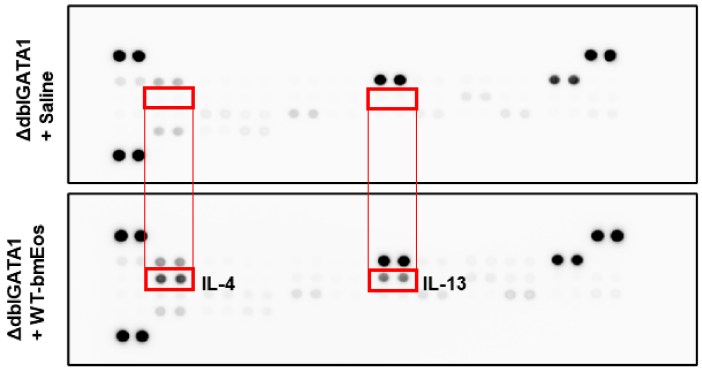

Fig. S6. Adoptive transfer of WT bmEos to ΔdblGATA-1 mice increased hepatic levels of IL-4 and IL-13. 6 Male ΔdblGATA-1 were subjected to hepatic IR surgery. After 24h, half of the mice were i.v. injected with bmEos ($10x10^6$) and the other half injected with saline as control. Mice were sacrificed after 3 days, and the expression levels of 40 cytokines in the liver samples were measured by using a Proteome Profiler Mouse Cytokine Array Kit. Data are representative of three independent experiments.

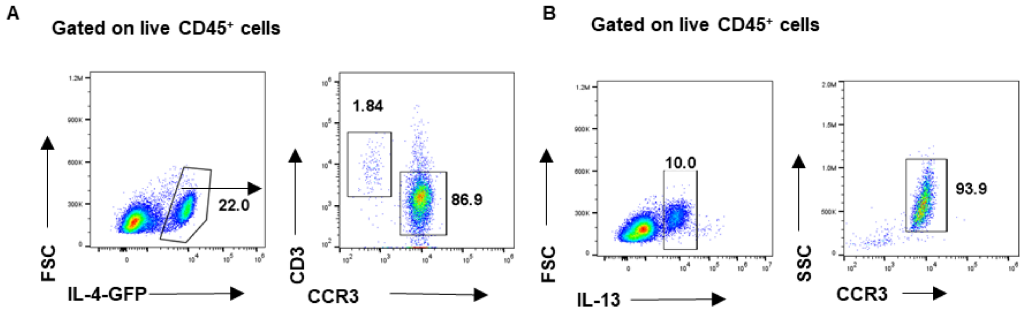

Fig. S7. IL-4 and IL-13 production by hepatic eosinophils during liver IR injury. (A, B) Male 4Get mice were subjected to hepatic IR injury and sacrificed after 3 days. Liver NPCs were isolated and stained intracellularly for IL-13. The IL-4-GFP$^+$ cells and IL-13$^+$ cells were gated. The proportions of IL-4$^+$ or IL-13$^+$ cells that were eosinophils (CCR3$^+$) are shown. Data are representative of three independent experiments.

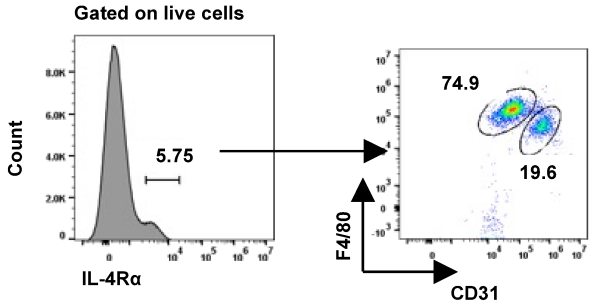

Fig. S8. Liver macrophages express IL-4Rα. Liver NPCs were isolated from naïve C57Bl/6J mice and analyzed by flow cytometry. IL-4Rα$^+$ cells were gated and identified as macrophages (F4/80$^+$, 74.9%) and LSECs (CD31$^+$, 19.6%). Data are representative of three independent experiments.

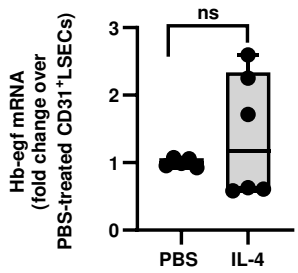

Fig.S9. IL-4 does not induce Hb-egf mRNA expression in liver sinusoidal endothelial cells (LSECs). LSECs were purified from naïve C57Bl/6J mice by magnetic-associated cell sorting (MACS) using anti-CD31 antibody. The cells were stimulated with IL-4 (10ng/ml) or PBS as the control for 6h (n=5-6/group). The mRNA levels of Hb-egf were measured by q-PCR. A two-tailed unpaired Student's t-test with Welch's correction was performed.

Table S1: Primer sequences for qRT-PCR

Gene Name (Symbol)	Forward Sequence	Reverse Sequence
Mouse Hb-egf	CGGGGAGTGCAGATACCTG	TTCTCCACTGGTAGAGTCAGC
Mouse Areg	GGTCTTAGGCTCAGGCCATTA	CGCTTATGGTGGAAACCTCTC
Mouse Tgf-α	CACTCTGGGTACGTGGGTG	CACAGGTGATAATGAGGACAGC
Mouse Btc	AATTCTCCACTGTGTGGTAGCA	GGTTTTCACTTTCTGTCTAGGGG
Mouse Ereg	CTGCCTCTTGGGTCTTGACG	GCGGTACAGTTATCCTCGGATTC
Mouse Epgn	GGGGGTTCTGATAGCAGTCTG	TCGGTGTTGTTAAATGTCCAGTT
Mouse Egf	AGAGCATCTCTCGGATTGACC	CCCGTTAAGGAAAACTCTTAGCA
Mouse 18s	ACGGAAGGGCACCACCAGGA	CACCACCACCCACGGAATCG